Supporting Information for

Impact of Labile Ligands on Catalyst Initiation and Chain Propagation in Ni-Catalyzed Ethylene/Acrylate Copolymerization

Shuoyan Xiong[a], Priyabrata Ghana[a], Brad C. Bailey[b], Heather A. Spinney[b], Briana S. Henderson[b], Matthew R. Espinosa[a], Theodor Agapie*[a]

*To whom correspondence should be addressed, E-mail: agapie@caltech.edu

[a]*Division of Chemistry and Chemical Engineering, California Institute of Technology, Pasadena, California 91125, United States*
[b]*Chemical Science, Core R&D, The Dow Chemical Company, Midland, Michigan 48667, United States*

Experimental details for

1. General Considerations

All air- and water-sensitive compounds were manipulated under N_2 or Ar using standard Schlenk or glovebox techniques. The solvents for air- and moisture-sensitive reactions were dried over sodium benzophenone/ketyl, calcium hydride, or by the method of Grubbs.[1] Deuterated solvents were purchased from Cambridge Isotopes Lab, Inc.; C_6D_6, was dried over a purple suspension with Na/benzophenone ketyl and vacuum transferred. tert-Butyl acrylate was dried over 4 Å sieves for greater than 72h. 2,4,6-Trimethylacetophenone was dried over 4 Å sieves for greater than 72h, vacuum transferred, and passed over an activated alumina plug. Acetophenone, dimethoxybenzene, and triethylphosphine were dried over calcium hydride and vacuum-transferred or distilled prior to use. Lithium bis(trimethylsilyl)amide (LiHMDS) were purchased from Sigma-Aldrich and used without further purification. Bis(dimethoxyphenyl)phosphine chloride, bis(diphenoxyphenyl)phosphine chloride, Metal precursor (tmeda)NiPhCl, phosphine enolate ligand ^{Ph}**PO**^{Ph}**H**, complex **2-PEt$_3$**, ^{Me}**PO**^{Ph}**-Ni(PEt$_3$)Ph**, ^{Ph}**PO**^{Mes}**-Ni(PEt$_3$)Ph**, ^{Ph}**PO**^{ArOMe}**-Ni(PEt$_3$)Ph**, ^{Ph}**PO**^{PhCF3}**-Ni(PEt$_3$)Ph**, and ^{Ph}**P*O**^{ArO}**-Ni(PEt$_3$)Ph** were synthesized according to literature procedures.[2-4] All ^{1}H, ^{13}C, and ^{31}P spectra of organic and organometallic compounds were recorded on Varian INOVA-400, or Bruker Cryoprobe 400 spectrometers. ^{1}H and ^{13}C chemical shifts are reported relative to residual solvent resonances.

2. Preparation of Metal Complexes

Synthesis of 2-bromo-4-tert-butyl-6-bis(2',6'-dimethoxyphenyl)phosphinophenol (^{MeO}POBrH)

A Schlenk flask fitted with a screw-in Teflon stopper was charged with a solution of 1,3-dibromo-5-(tert-butyl)-2-(methoxymethoxy)benzene (3.52 g, 10.0 mmol) in THF (40 mL) and cooled to -78 °C under nitrogen. A hexane solution of n-butyllithium (4 mL, 2.5 M, 10.0 mmol) was added dropwise via syringe. After stirring for an additional 30 min at -78 °C, a solution of bis(2,6-dimethoxyphenyl)phosphine chloride (3.41 g, 10.0 mmol) in THF (20 mL) was added dropwise via cannula. After complete addition, the reaction was allowed to warm up to room temperature and stirred for an additional 3 h, yielding a yellow solution. The solution was then concentrated to ~20 mL. Degassed MeOH (10 mL) was added, followed by the addition of concentrated aqueous HCl (5 mL). The resulting mixture was degassed immediately via three freeze-pump-thaw cycle with a liquid nitrogen bath. After stirring for 4 h under room temperature, volatiles were removed under vacuum. In a N_2-filled glovebox (no exclusion of water), the resulting pale-yellow residue was taken up in CH_2Cl_2 (40 mL), washed with saturated aqueous solutions of K_2CO_3 (3 x 10 mL) and NH_4Cl (3 x 10 mL), dried over $MgSO_4$, and filtered through Celite. The volatiles were removed under reduced pressure. In a glovebox (exclusion of water and oxygen), the resulting pale-yellow solid was dissolved in ether and filtered through Celite. The volatile materials were removed once more under vacuum and the resulting mixture was washed by hexanes (10 mL) and the solid was collected via vacuum filtration. Further recrystallization from cold, concentrated Et_2O solution yields 2-bromo-4-tert-butyl-6-bis(2',6'-dimethoxyphenyl)phosphinophenol (^{MeO}**POBrH**, 4.05 g, 70% yield) as a white powder. ^{1}H NMR (400 MHz, C_6D_6): δ 7.97 (dd, *J* = 13.0, 2.5 Hz, 1H, ArH), 7.80 (d, *J* = 2.4 Hz, 1H, OH), 7.62 (d, *J* = 2.4 Hz, 1H, ArH), 7.0 (dt, *J* = 8.3, 1.1 Hz, 2H, ArH), 6.20 (dd, *J* = 8.3, 2.9 Hz, 4H, ArH), 3.14 (s, 12H, OCH_3), 1.15 (s, 9H, $C(CH_3)_3$). ^{13}C{^{1}H} NMR (101 MHz, C_6D_6): δ 161.89 (d, *J* = 8.4 Hz, 4C, Aryl-C), 153.94 (d, *J* = 4.8 Hz, 1C, Aryl-C), 142.51 (d, *J* = 12.8 Hz, 1C, Aryl-C), 132.64 (d, *J* = 42.0 Hz, 1C, Aryl-C), 130.71 (s, 1C, Aryl-C), 129.79 (s, 2C, Aryl-C), 125.48 (d, *J* = 17.2 Hz, 1C, Aryl-C), 112.91 (d, *J* = 22.7 Hz, 2C, Aryl-C), 109.38 (s, 1C, Aryl-C), 104.25 (s, 4C, Aryl-C), 55.26 (s, 4C, OCH_3), 34.08 (s, 1C, $\underline{C}(CH_3)_3$), 31.51 (s, 3C, $C(\underline{C}H_3)_3$). ^{31}P{^{1}H} NMR (162 MHz, C_6D_6) δ -55.2 (s).

Synthesis of ^{MeO}POBr-Ni(PEt$_3$)Ph (1-PEt$_3$)

In a Schlenk tube, a solid mixture of **^{MeO}POBrH** (75 mg, 0.14 mmol) and $LiCH_2SiMe_3$ (13 mg, 0.14 mmol) was treated with cold (+5 °C) benzene (8 mL). The resulting mixture was slowly warmed to room temperature and stirred for an additional 1 hour. To this reaction mixture, a benzene solution (2 mL) of [NiCl(Ph)(PEt_3)$_2$] (53 mg, 0.14 mmol, 1 equiv.) was added at room temperature. The resulting yellow suspension was heated to 80 °C for 18 hours under nitrogen atmosphere. After completion of the reaction, as confirmed by an aliquot ^{31}P NMR, the reaction mixture was filtered into a 20 mL glass vial, and the yellow filtrate was evaporated to dryness under reduced pressure. The resulting residue was washed with hexane (3 × 5 mL) at room temperature and dried under reduced pressure for 3 hours to obtain **1-PEt$_3$** as an analytically pure yellow solid. Yield: 90 mg (0.11 mmol, 82%).

^{1}H NMR (400 MHz, C_6D_6): δ 7.73 (dd, *J* = 9.9, 1.7 Hz, 1H, ArH), 7.61 (d, *J* = 1.7 Hz, 1H, ArH), 7.19 (d, *J* = 7.3 Hz, 2H, ArH), 7.02 (t, *J* = 8.3 Hz, 2H, ArH), 7.62 (t, *J* = 7.2 Hz, 2H, ArH), 6.62 (t, *J* = 7.2 Hz, 1H, ArH), 6.18 (dd, $^3J_{H,H}$ = 8.4 Hz, $^4J_{H,P}$ = 3.4 Hz, 4H, ArH), 3.18 (s, 12H, -OC*H*$_3$), 1.49 (m, 6H, PC*H*$_2$), 1.18 (m, 9H, PCH_2CH_3), 1.14 (s, 9H, $C(CH_3)_3$). ^{13}C{^{1}H} NMR (101 MHz, C_6D_6): δ 168.75 (dd, *J* = 30.4, 7.4 Hz, 2C, Aryl-C), 161.56 (s, 4C, Aryl-C), 151.59 (dd, *J* = 32.4, 7.4 Hz, 2C, Aryl-C), 137.27 (t, *J* = 3.7 Hz, 2C, Aryl-C), 136.11 (d, *J* = 6.5 Hz, 1C, Aryl-C), 131.34 (d, *J* = 1.5 Hz, 1C, Aryl-C), 130.32 (s, 2C, Aryl-C), 127.09 (d, *J* = 2.2 Hz, 1C, Aryl-C), 125.63 (d, *J* = 49.4 Hz, 1C, Aryl-C), 125.02 (t, *J* = 2.5 Hz, 2C, Aryl-C), 120.09 (t, *J* = 2.2 Hz, 1C, Aryl-C), 113.46 (d, *J* = 14.8 Hz, 1C, Aryl-C), 110.54 (dd, *J* = 45.2, 1.8 Hz, 2C, Aryl-C), 104.20 (d, *J* = 4.2 Hz, 4C, Aryl-C), 55.48 (s, 4C, OCH_3), 33.80 (s, 1C, $\underline{C}(CH_3)_3$), 31.92 (s, 3C, $C(\underline{C}H_3)_3$), 13.94 (d, J = 22.0 Hz, 3C, $P\underline{C}H_2CH_3$), 8.28 (s, 3C, $PCH_2\underline{C}H_3$). ^{31}P{^{1}H} NMR (162 MHz, C_6D_6) δ 15.0 (d, *J* = 298.8 Hz, 1P), -3.6 (d, *J* = 298.8 Hz, 1P). Anal. Calcd(%) for $C_{38}H_{49}BrNiO_5P_2$: C: 58.04, H: 6.28; found: C: 58.87, H: 6.34.

Synthesis of ^{MeO}POBr-Ni(py)Ph (1-py)

In the glove box, to a precooled (-78 °C) solution of the ligand **^{MeO}POBrH** (107 mg, 0.2 mmol) in tetrahydrofuran (THF) (2 mL) was added a precooled (-78 °C) solution (2 mL) of LiHMDS (33.4 mg, 0.2

mmol) in THF. The mixture was then slowly warmed up to room temperature and stirred for 8 h at room temperature. All volatiles were removed from solution which was triturated with pentane (2 x 5 mL). The resulting residue was dissolved in toluene (4 mL) and cooled to -78 °C. To this solution was added a toluene solution (2 mL) of (tmeda)NiPhCl (57.2 mg, 0.2 mmol) and pyridine (79 mg, 1.0 mmol). The mixture was then slowly warmed up to room temperature and stirred for additional 24 h. Next, the mixture was filtered through Celite and volatiles were removed under vacuum. The resulting solids were further washed with pentane (5~10 mL*3), hexanes (1 mL), and diethyl ether (1 mL), yielding metal complexes (**1-py**) as analytically pure yellow solids (97 mg, yield: 65%).

^{1}H NMR (400 MHz, C_6D_6): δ 8.95 – 8.89 (m, 2H, ArH), 7.71 (d, *J* = 2.3 Hz, 1H, ArH), 7.66 (dd, *J* = 11.3, 2.4 Hz, 1H, ArH), 7.60 (d, *J* = 7.2 Hz, 2H, ArH), 7.02 (t, *J* = 8.3 Hz, 2H, ArH), 6.82 (t, *J* = 7.2 Hz, 2H, ArH), 6.78 – 6.73 (m, 1H, ArH), 6.71-6.67 (m, 1H, ArH), 6.42 (t, *J* = 6.4 Hz, 2H, ArH), 6.17 (dd, *J* = 8.3, 3.8 Hz, 4H, ArH), 3.17 (s, 12H, -OCH_3), 1.14 (s, 9H, -*t*Bu). ^{13}C{^{1}H} NMR (101 MHz, C_6D_6): δ 167.38 (d, *J* = 23.5 Hz, 2C, ArC), 161.51 (s, 4C, ArC), 155.34 (d, *J* = 48.0 Hz, 1C, ArC), 151.81 (s, 2C, ArC), 138.35 (s, 2C, ArC), 136.47 (s, 1C, ArC), 136.12 (d, *J* = 6.9 Hz, 1C, ArC), 131.58 (s, 1C, ArC), 130.79 (s, 2C, ArC), 126.88 (s, 1C, ArC), 126.46 (s, 1C, ArC), 125.42 (s, 2C, ArC), 123.51 (s, 2C, ArC), 121.30 (s, 1C, ArC), 112.96 (d, *J* = 16.2 Hz, 1C, ArC), 110.05 (d, *J* = 54.5 Hz, 1C, ArC), 104.18(s, 4C, ArC), 55.36 (s, 4C, -OMe), 33.86 (s, 1C, -$\underline{C}(CH_3)_3$), 31.98 (s, 3C, -$C(\underline{C}H_3)_3$). ^{31}P{^{1}H} NMR (162 MHz, C_6D_6) δ -0.63 (s). Anal. Calcd(%) for $C_{37}H_{38}BrNNiO_5P$: C: 59.47, H: 5.26, N: 1.87; found: C: 60.37, H: 5.40, N: 2.13.

Synthesis of $^{Ph}PO^{Ph}$-Ni(py)Ph (2-py)

In the glove box, to a precooled (-78 °C) solution of the ligand **$^{Ph}PO^{Ph}H$** (134.4 mg, 0.2 mmol) in tetrahydrofuran (THF) (2 mL) was added a precooled (-78 °C) solution (2 mL) of LiHMDS (33.4 mg, 0.2 mmol) in THF. The mixture was then slowly warmed up to room temperature and stirred for 8 h at room temperature. All volatiles were removed from solution which was triturated with pentane (2 x 5 mL). The resulting residue was dissolved in toluene (4 mL) and cooled to -78 °C. To this solution was added a

toluene solution (2 mL) of (tmeda)NiPhCl (57.2 mg, 0.2 mmol) and pyridine (79 mg, 1.0 mmol). The mixture was then slowly warmed up to room temperature and stirred for additional 24 h. Next, the mixture was filtered through Celite and volatiles were removed under vacuum. After washed with pentane (5~10 mL*3), hexanes (1 mL), and cold diethyl ether (2 mL), the resulting solids was further purified by precipitation from cold, concentrated solution in diethyl ether, yielding metal complexes (**2-py**) as yellow-brownish solids (44 mg, yield: 25%).

^{1}H NMR (400 MHz, C_6D_6) δ 8.08 – 7.98 (m, 4H, 4ArH), 7.49 (dd, J = 7.6, 2.0 Hz, 2H, 2ArH), 7.12 – 7.06 (m, 3H, ArH), 7.03 – 6.94 (m, 11H, ArH), 6.95 – 6.88 (m, 8H, ArH), 6.85 – 6.80 (m, 4H, ArH), 6.75 (t, J = 8.2 Hz, 2H, ArH), 6.69 – 6.64 (m, 1H, ArH), 6.60-6.55 (m, 1H, ArH), 6.47 (dd, J = 8.2, 3.3 Hz, 4H, ArH), 6.21-6.16 (m, 2H, ArH), 5.23 (broad s, 1H, -C<u>H</u>C(O)-). ^{13}C{^{1}H} NMR (101 MHz, C_6D_6): δ 177.67 (d, J = 20.7 Hz), 159.16 (s), 158.10 (s), 155.82 (d, J = 44.3 Hz), 151.22(s). 140.14 (d, J = 15.6 Hz), 138.76 (s), 136.00 (s), 130.12 (s), 129.76(s), 127.80 (s), 127.61 (s), 127.42 (s), 125.75 (s), 123.09 (s), 122.96 (s), 121.73 (s), 120.49 (s), 119.82 (s), 113.73 (s), 82.45 (d, J = 58.7 Hz). ^{31}P{^{1}H} NMR (162 MHz, C_6D_6) δ -2.63 (s). Anal. Calcd(%) for $C_{55}H_{42}NNiO_5P$: C: 74.51, H: 4.78, N: 1.58; Found (%): C, 74.15; H, 5.07; N, 1.17.

Synthesis of $^{Ph}PO^{Ph}$-Ni(PPh$_3$)Ph (2-PPh$_3$)

In the glove box, to a solution of **2-py** (35.44 mg, 0.04 mmol) in toluene (6 mL) was added 1 equiv. of PPh_3 (10.48 mg, 0.04 mmol). After stirring for 15 min, all volatiles were removed under vacuum. To the residue was added toluene (6 mL) and the volatiles were removed under vacuum again. The above step was repeated for several times until quantitative converion of **2-py** to **2-PPh$_3$** (41.8 mg, >97% yield).

^{1}H NMR (400 MHz, C_6D_6) δ 7.50 (ddd, J = 9.8, 7.7, 1.8 Hz, 8H, ArH), 7.08 – 6.88 (m, 30H, ArH), 6.87 – 6.81 (m, 4H, Raha), 6.73 – 6.66 (m, 3H, ArH), 6.60 (t, J = 7.7 Hz, 2H, ArH), 6.42 (dd, J = 8.2, 3.2 Hz, 4H, ArH), 5.18 (d, J = 1.7 Hz, 1H, ArH). ^{31}P NMR (162 MHz, C_6D_6) δ -5.98 (d, *J* = 303 Hz), 23.44 (d, *J* = 303 Hz).

3. Ligand Exchange Studies

Representative procedure. In the glovebox, to a solution of **2-PEt$_3$** (0.0059 mmol, 5.5 mg) and in C_6D_6 (438 mg) was added a known amount of pyridine. The mixture was fully dissolved and transferred to an NMR tube. The rate of exchange is slow relative to the NMR timescale which lead to two separate species observed. $^{31}P\{^1H\}$ and ^1H NMR spectra were collected in 1-h intervals until the spectra remained unchanged. The relative intensities of the two species are determined through the $^{31}P\{^1H\}$ NMR resonances.

Results.

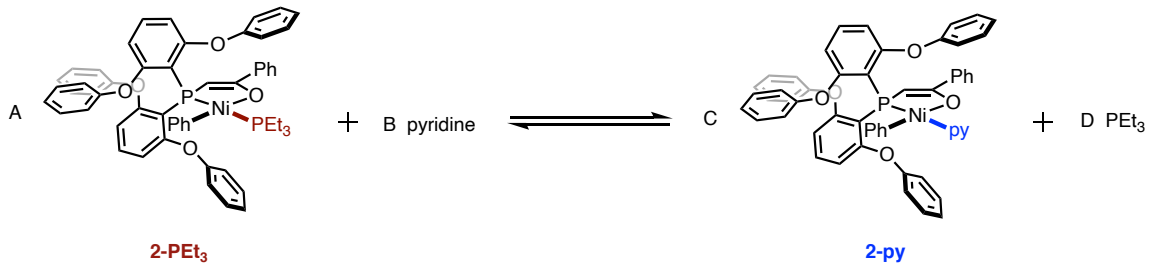

2-PEt$_3$ **2-py**

Entry	A_0	B_0	$A_{Equilbrium}$	$B_{Equilbrium}$	$C_{Equilbrium}$	$D_{Equilbrium}$	$K_{py/PEt3}$	$\mathbf{K_{PEt3/py}}$
1	1	150	0.92	~150	0.08	0.08	0.0000464	**21600**
2	1	1000	0.80	~1000	0.20	0.20	0.000050	**20000**
3	1	1500	0.76	~1500	0.24	0.24	0.0000505	**19800**

Therefore $K_{P/py}$~ 20000, log $K_{PEt3/py}$~ 4.3.

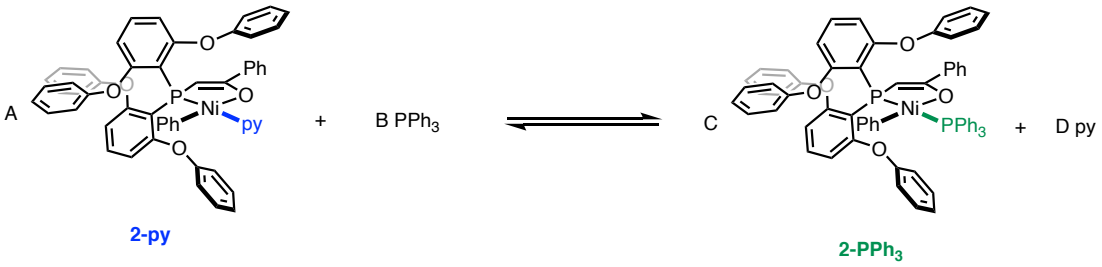

2-py **2-PPh$_3$**

Entry	A_0	B_0	C_0	D_0	$A_{Equilbrium}$	$B_{Equilbrium}$	$C_{Equilbrium}$	$D_{Equilbrium}$	$\mathbf{K_{PPh3/py}}$
1	1	1	0	0	0.35	0.35	0.65	0.65	**3.4**
2	1	2	0	0	0.15	1.15	0.85	0.85	**4.2**
3	1	4	1	1	0.14	3.14	0.86	1.86	**3.6**

Therefore $K_{P/py}$~ 4, log $K_{PPh3/py}$~ 0.6.

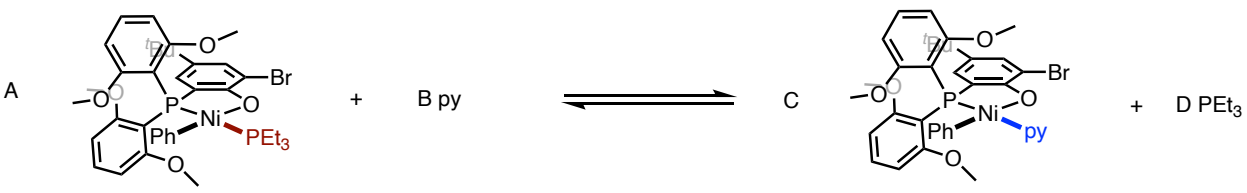

1-PEt$_3$ **1-py**

Entry	A_0	B_0	$A_{Equilbrium}$	$B_{Equilbrium}$	$C_{Equilbrium}$	$D_{Equilbrium}$	$K_{py/PEt3}$	$\mathbf{K_{PEt3/py}}$
1	1	200	0.92	~200	0.08	0.08	0.0000348	**28800**
2	1	500	0.87	~500	0.13	0.13	0.0000388	**25800**
3	1	3000	0.71	~3000	0.29	0.29	0.0000395	**25326**

Therefore $K_{P/py}$~ 25000, log $K_{PEt3/py}$~ 4.4.

4 NMR Spectra

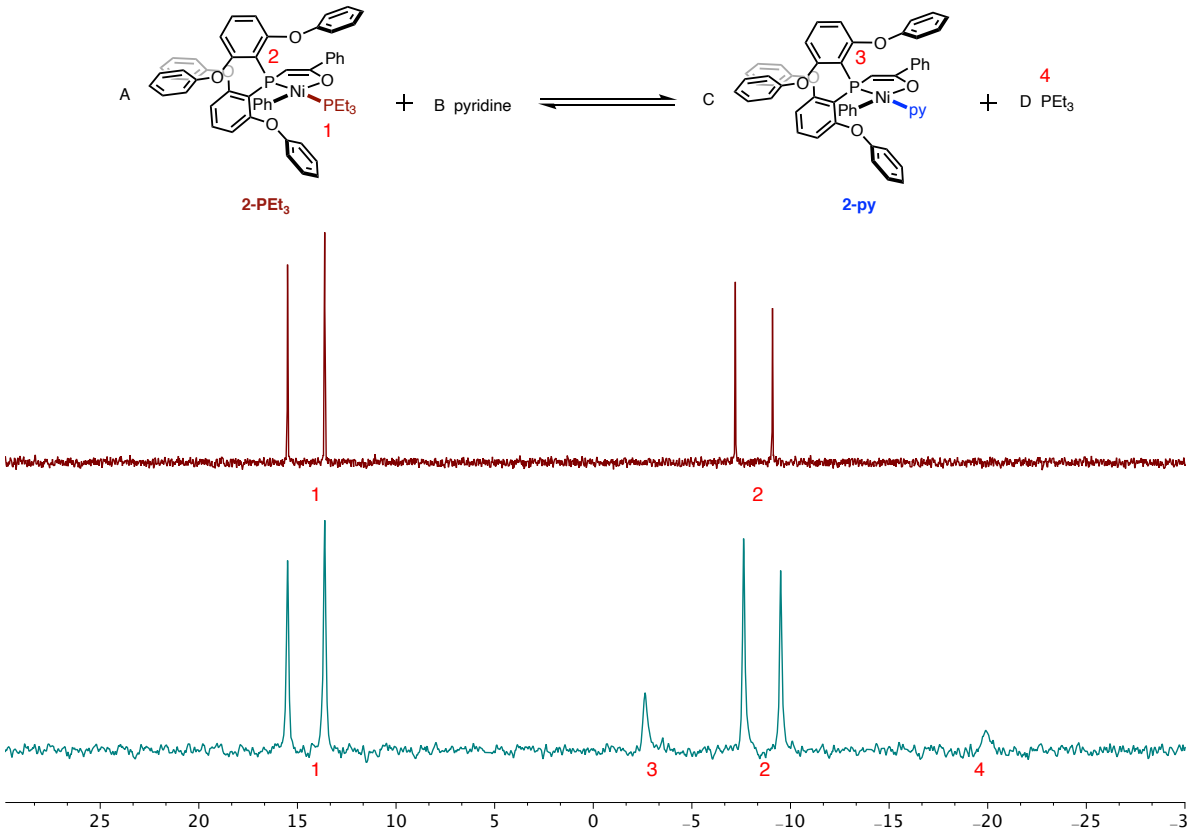

Figure S1. Representative $^{31}P\{^{1}H\}$ NMR spectra for exchange studies. Top/Red spectrum: **2-PEt$_3$** (in C_6D_6); Bottom/Green spectrum: Mixtures upon addition of excess pyridine to **2-PEt$_3$** (Condition: **2-PEt$_3$**: 0.0059 mmol, pyridine: 5.9 mmol, no additional solvent, T: 25 °C).

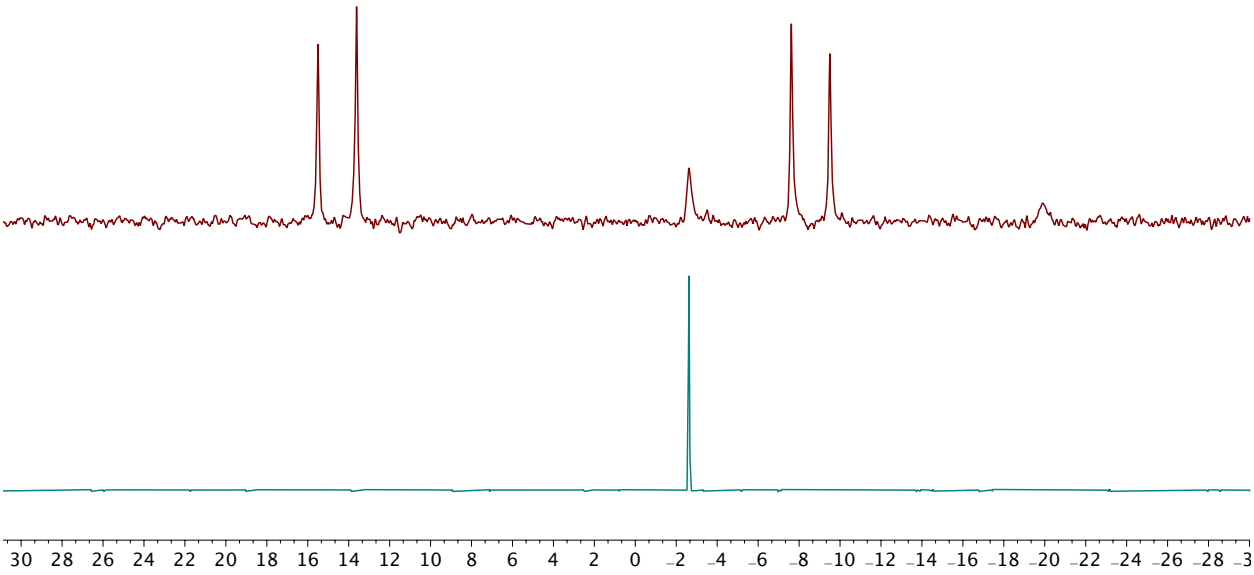

Figure S2. Comparison of mixture generated in exchange studies (Top/Red spectrum, also shown as the bottom spectrum in Figure S1) and independently synthesized **2-py** (bottom/Green spectrum, in C_6D_6).

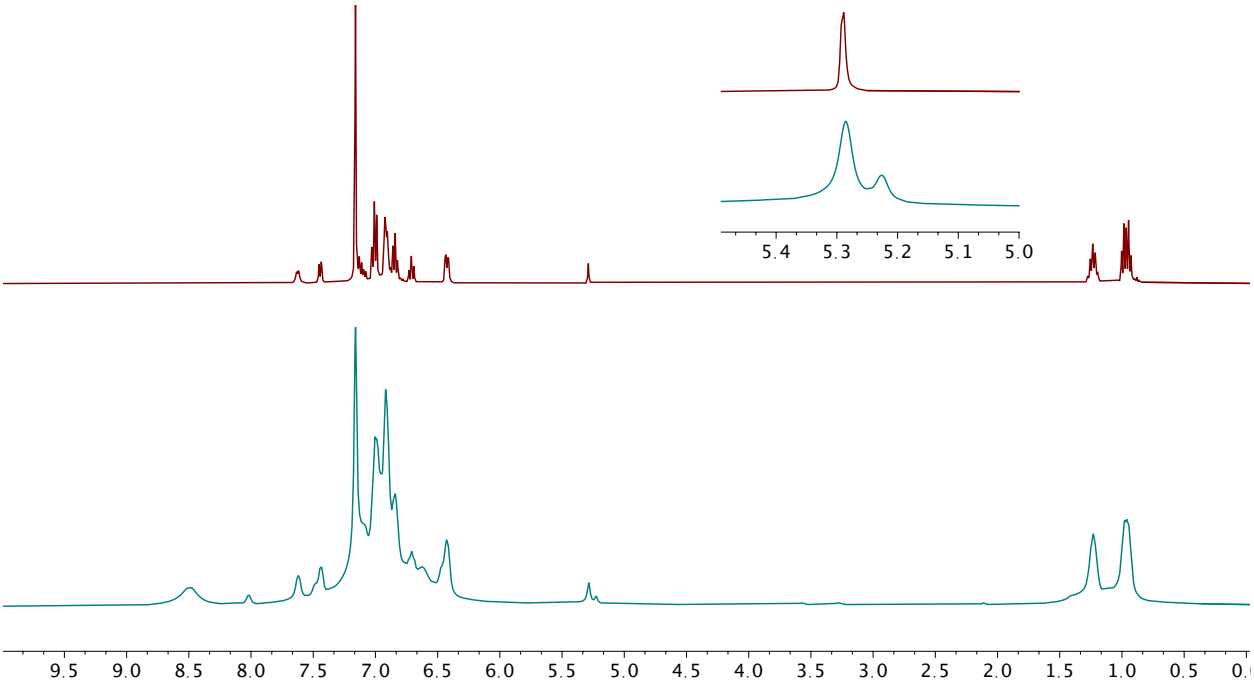

Figure S3. Comparison of **2-PEt$_3$** (Top/Red spectrum, in C_6D_6) and mixture generated in exchange studies (Bottom/Green spectrum, condition: To the benzene solution of **2-PEt$_3$** was added 1500 equiv. of pyridine, the mixture was then stirred overnight, and volatiles were then removed.

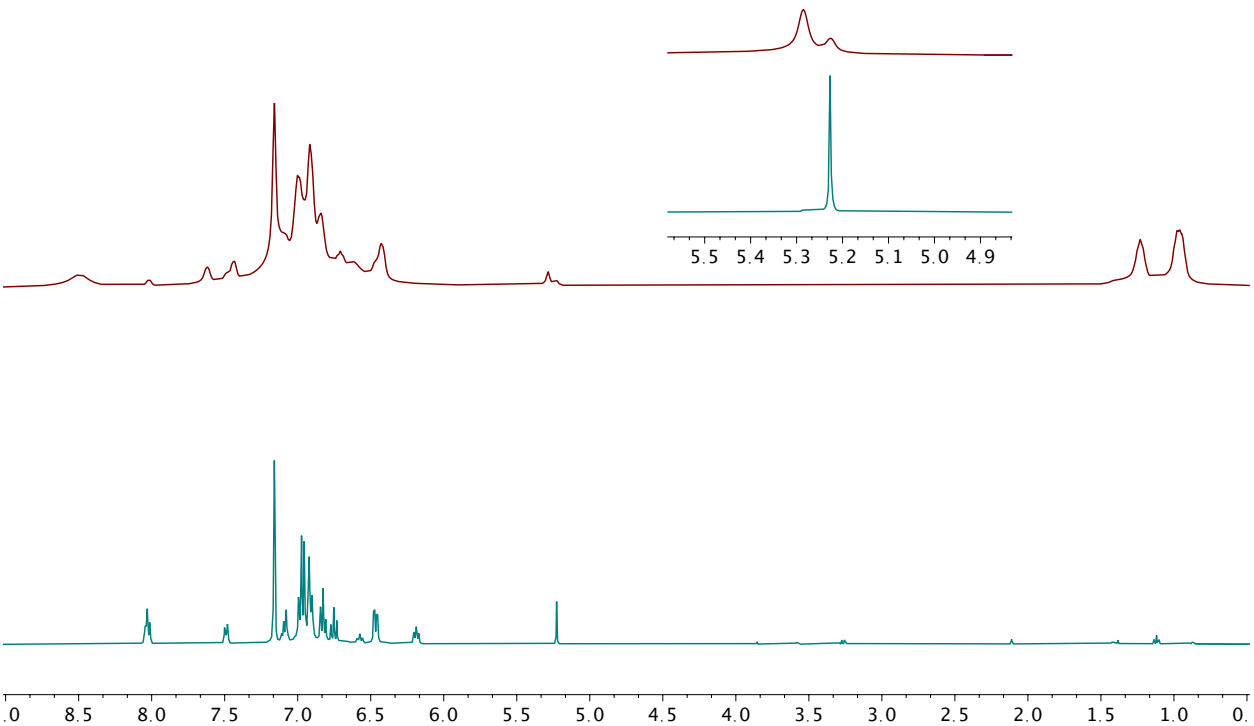

Figure S4. Comparison of mixture generated in exchange studies (Top/Red spectrum, also shown as the bottom spectrum in Figure S3) and **2-py** (Bottom/Green spectrum, in C_6D_6).

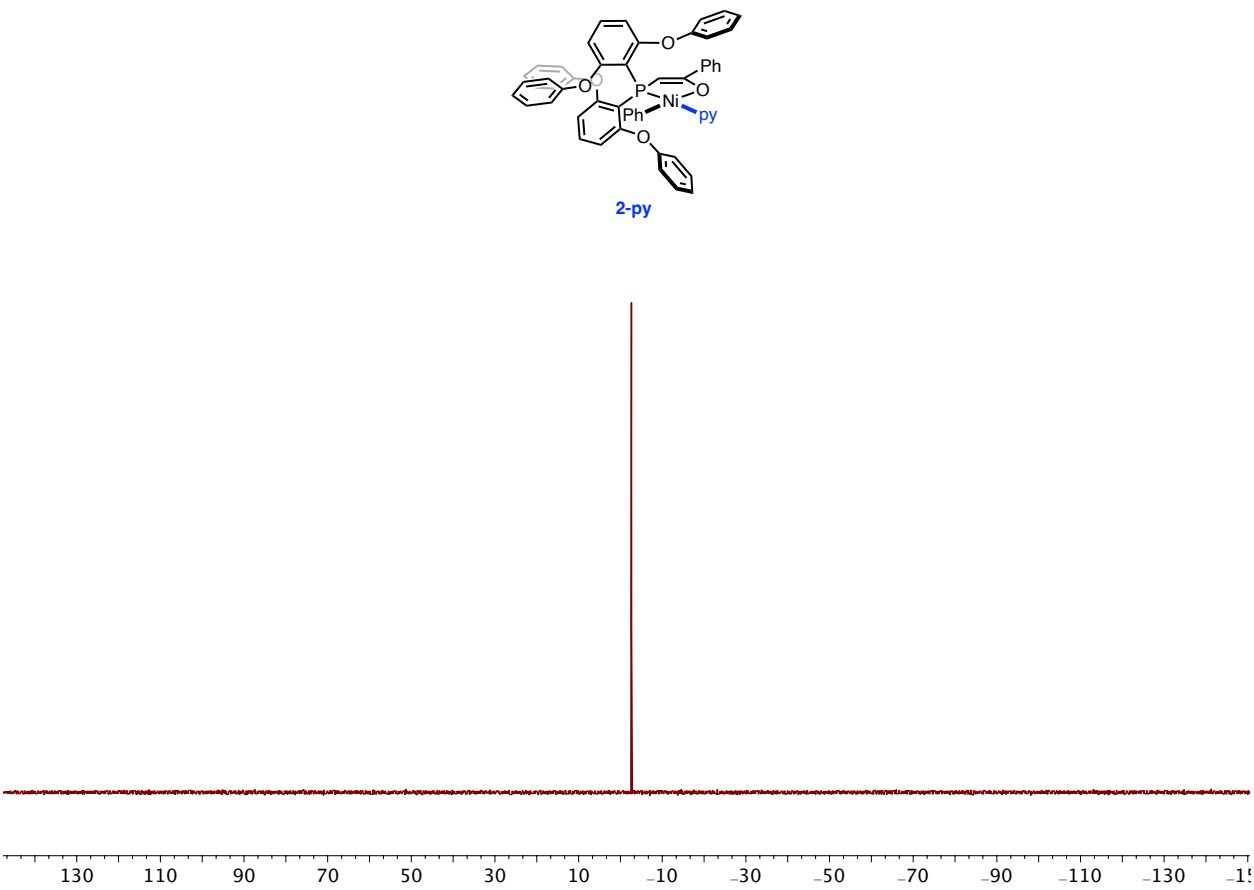

Figure S5. $^{31}P\{^{1}H\}$ NMR spectrum of **2-py** in C_6D_6.

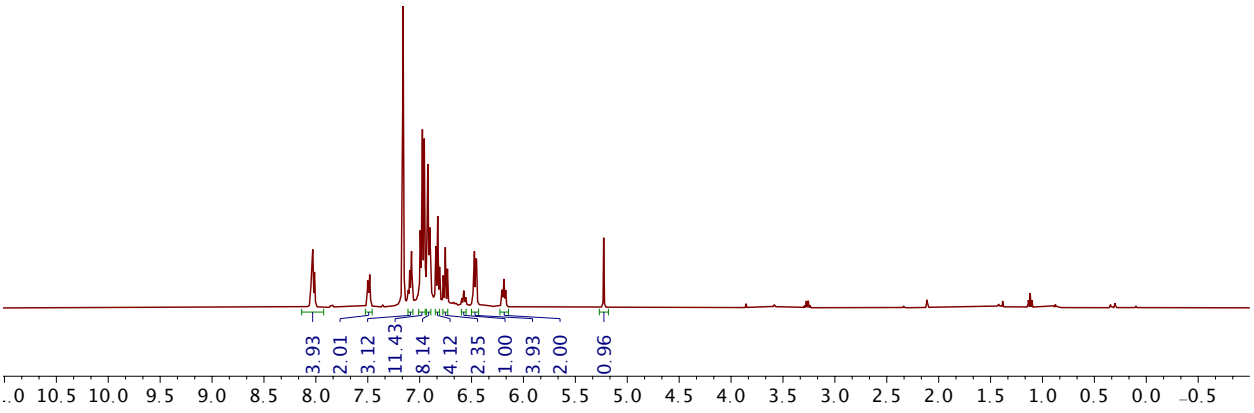

Figure S6. ^{1}H NMR spectrum of **2-py** in C_6D_6.

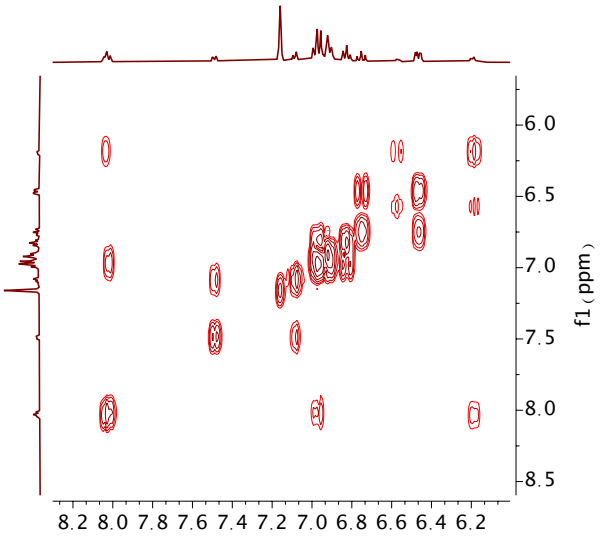

Figure S7. ^{1}H-^{1}H COSY NMR spectrum of **2-py** in C_6D_6.

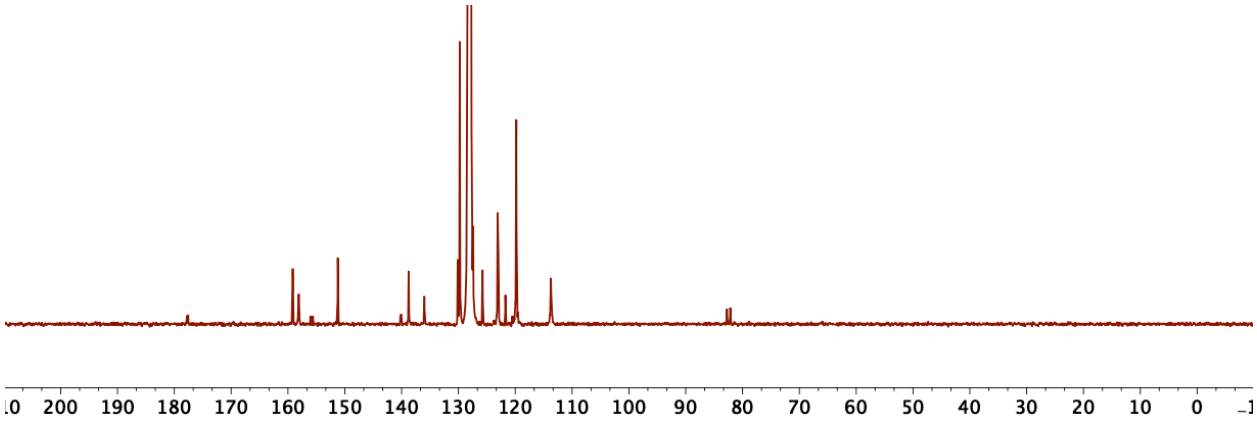

Figure S8. $^{13}C\{^{1}H\}$ NMR spectrum of **2-py** in C_6D_6.

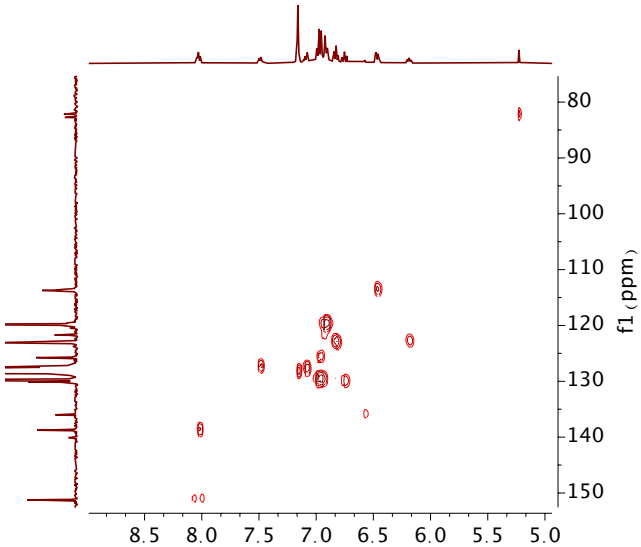

Figure S9. ^{1}H-^{13}C HSQC NMR spectrum of **2-py** in C_6D_6.

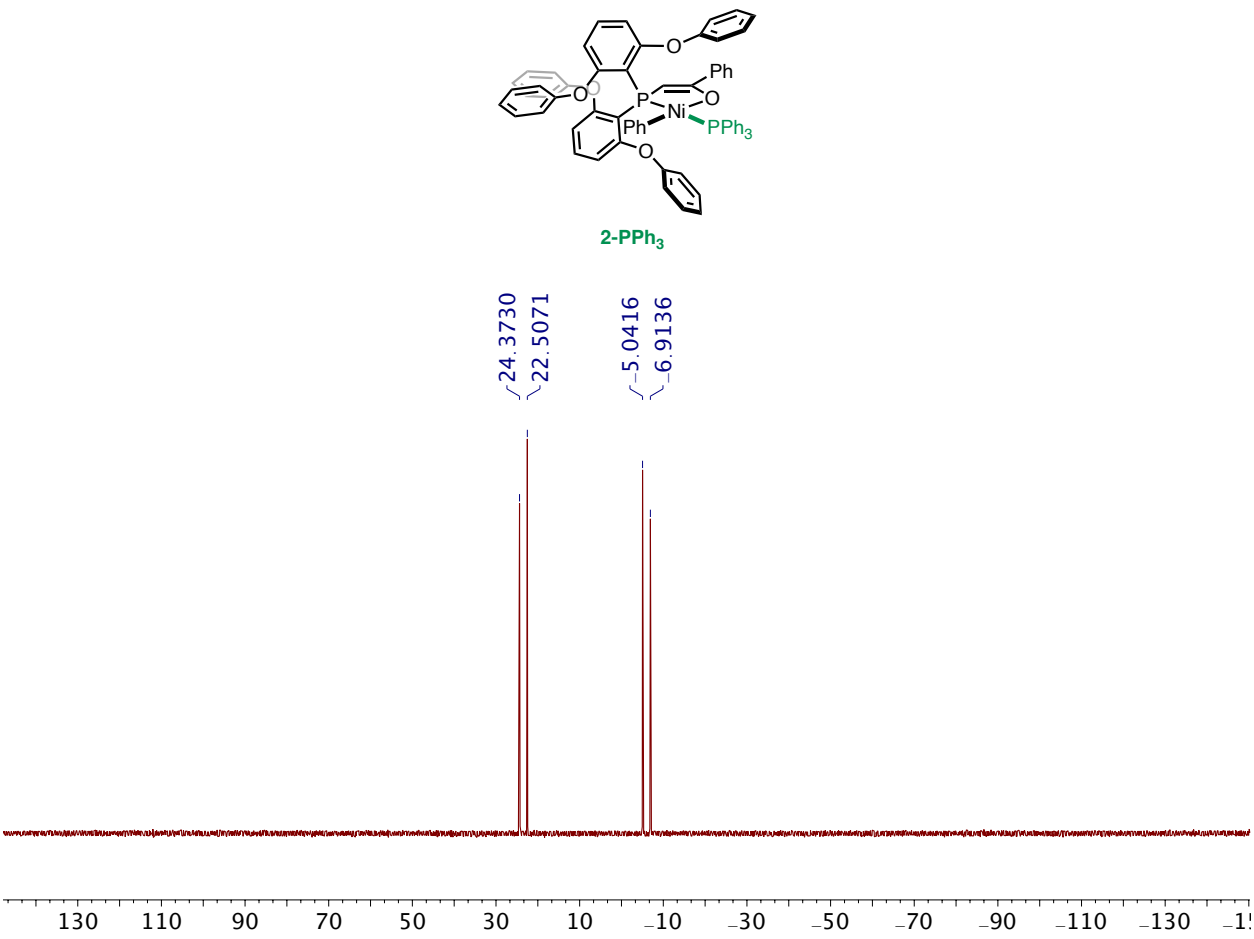

Figure S10. $^{31}P\{^{1}H\}$ NMR spectrum of **2-PPh$_3$** in C_6D_6.

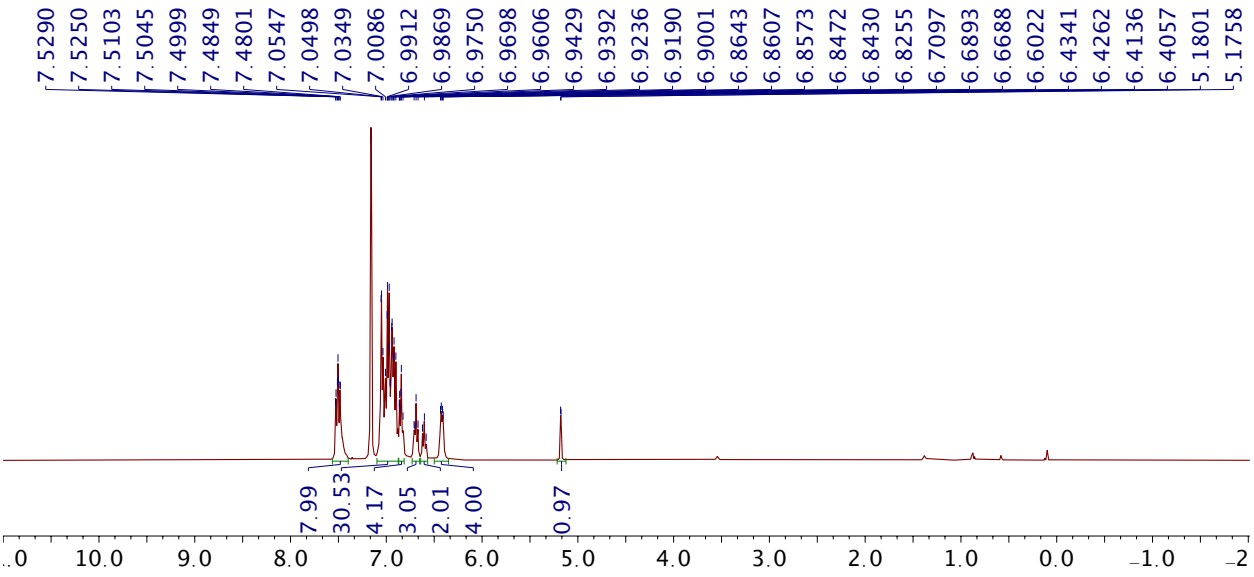

Figure S11. ^{1}H NMR spectrum of **2-PPh$_3$** in C_6D_6.

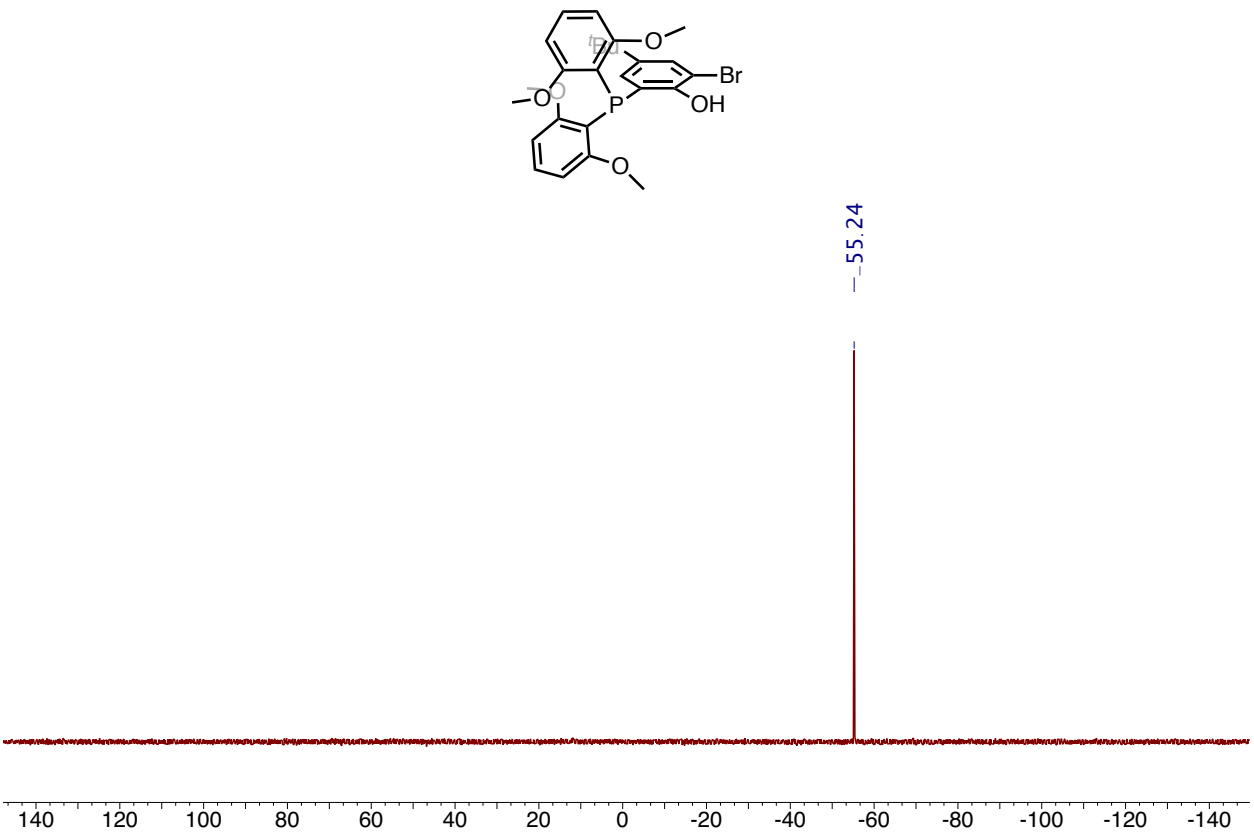

Figure S12. $^{31}P\{^{1}H\}$ NMR spectrum of ^{MeO}**POBrH** in C_6D_6.

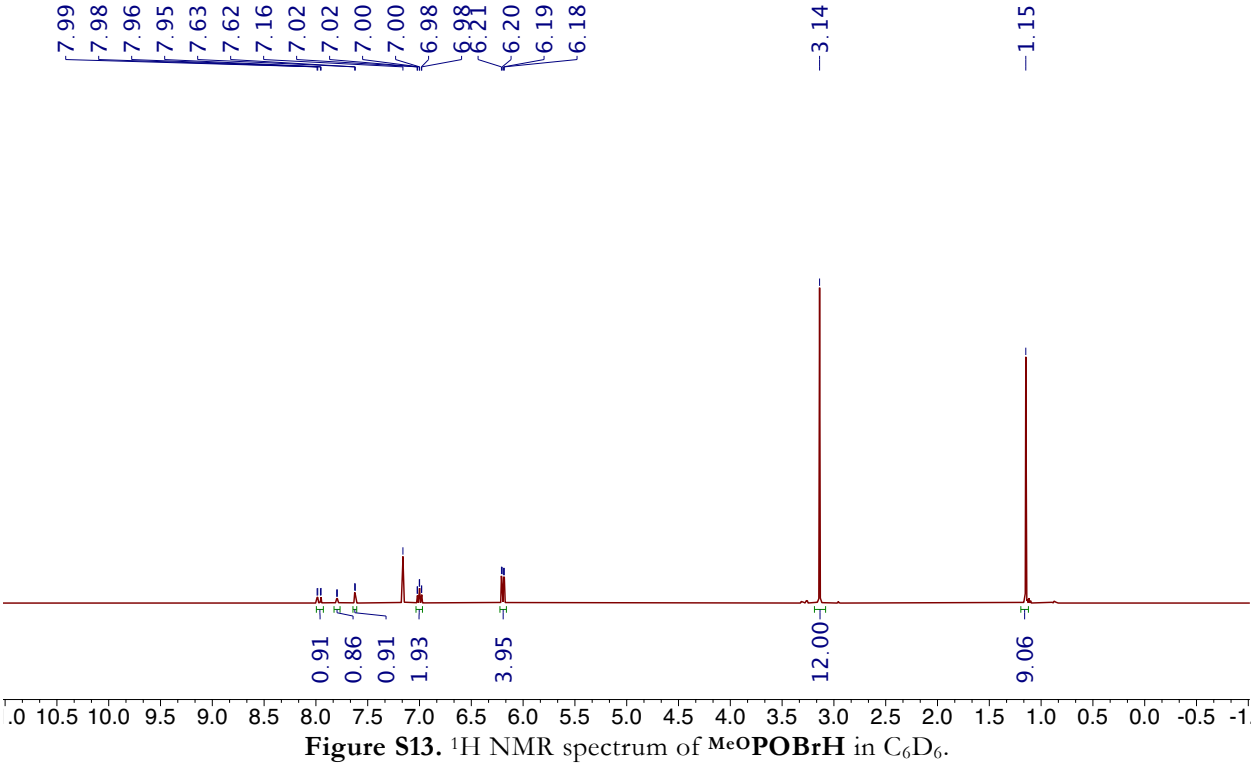

Figure S13. ^{1}H NMR spectrum of ^{MeO}**POBrH** in C_6D_6.

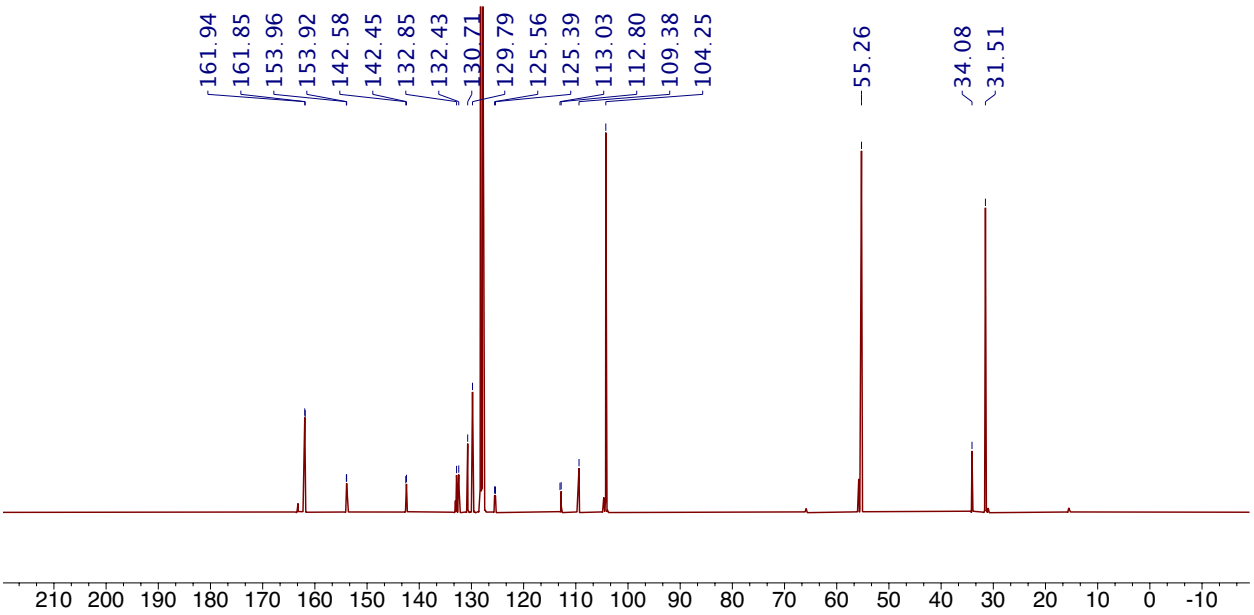

Figure S14. $^{13}C\{^{1}H\}$ NMR spectrum of ^{MeO}**POBrH** in C_6D_6.

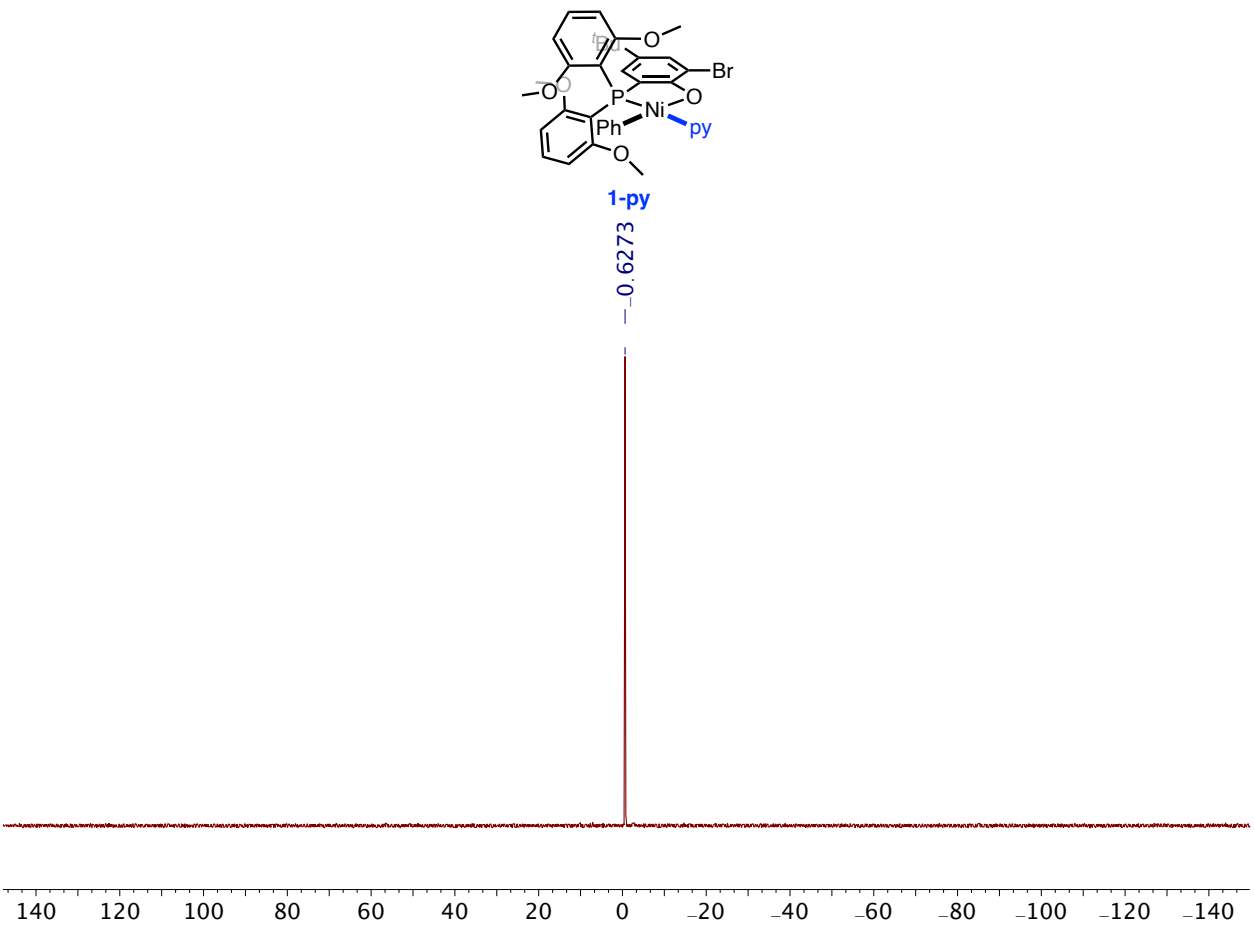

Figure S15. $^{31}P\{^{1}H\}$ NMR spectrum of **1-py** in C_6D_6.

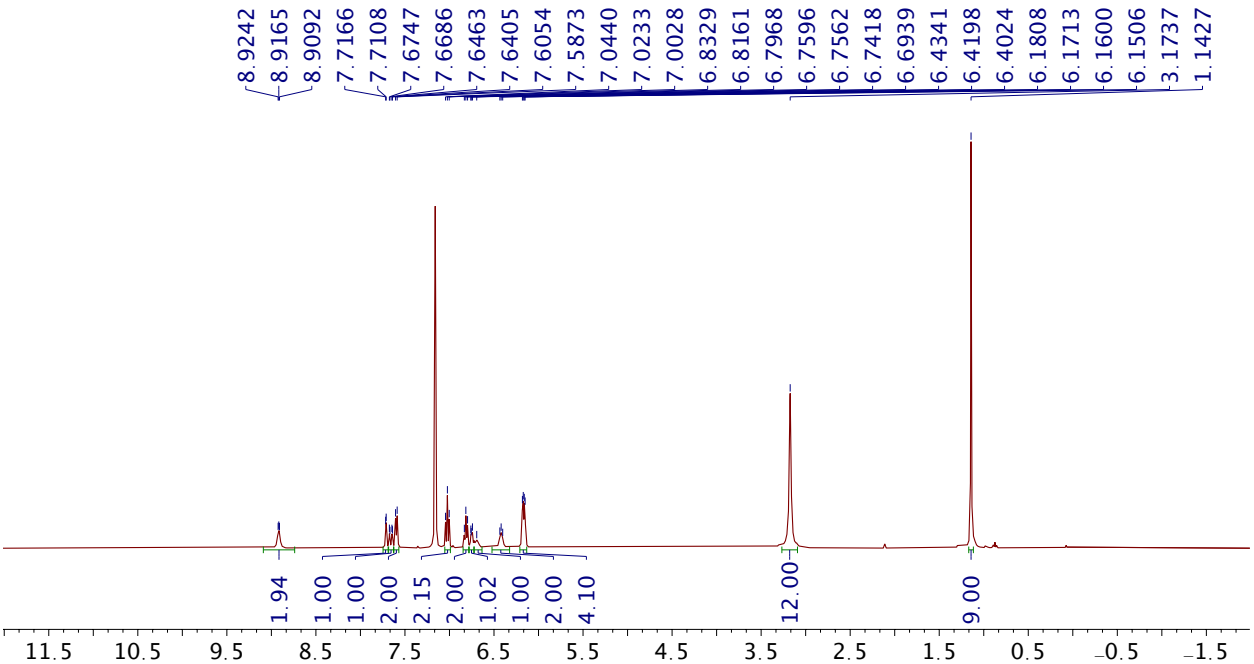

Figure S16. ^{1}H NMR spectrum of **1-py** in C_6D_6.

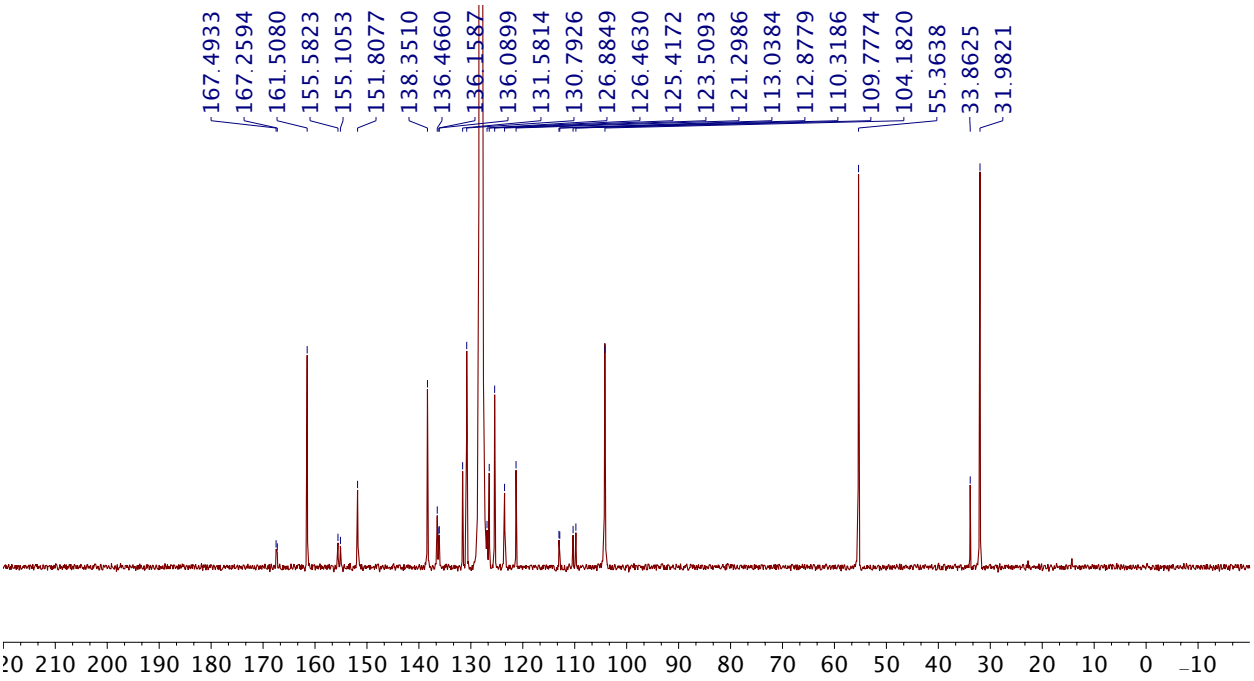

Figure S17. $^{13}C\{^{1}H\}$ NMR spectrum of **1-py** in C_6D_6.

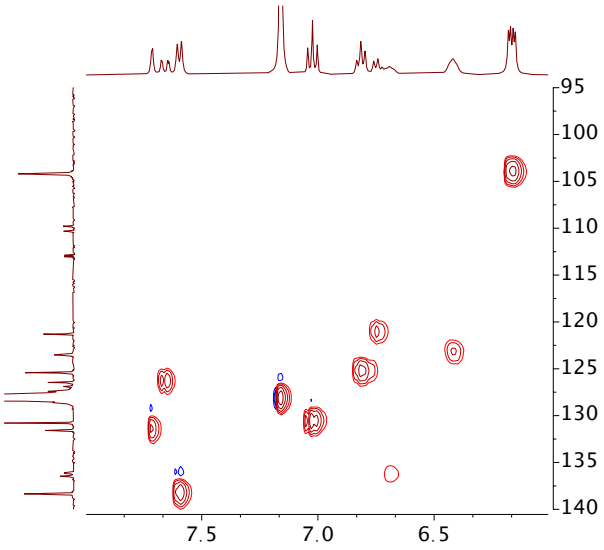

Figure S18. ^{1}H-^{13}C HSQC NMR spectrum of **1-py** in C_6D_6.

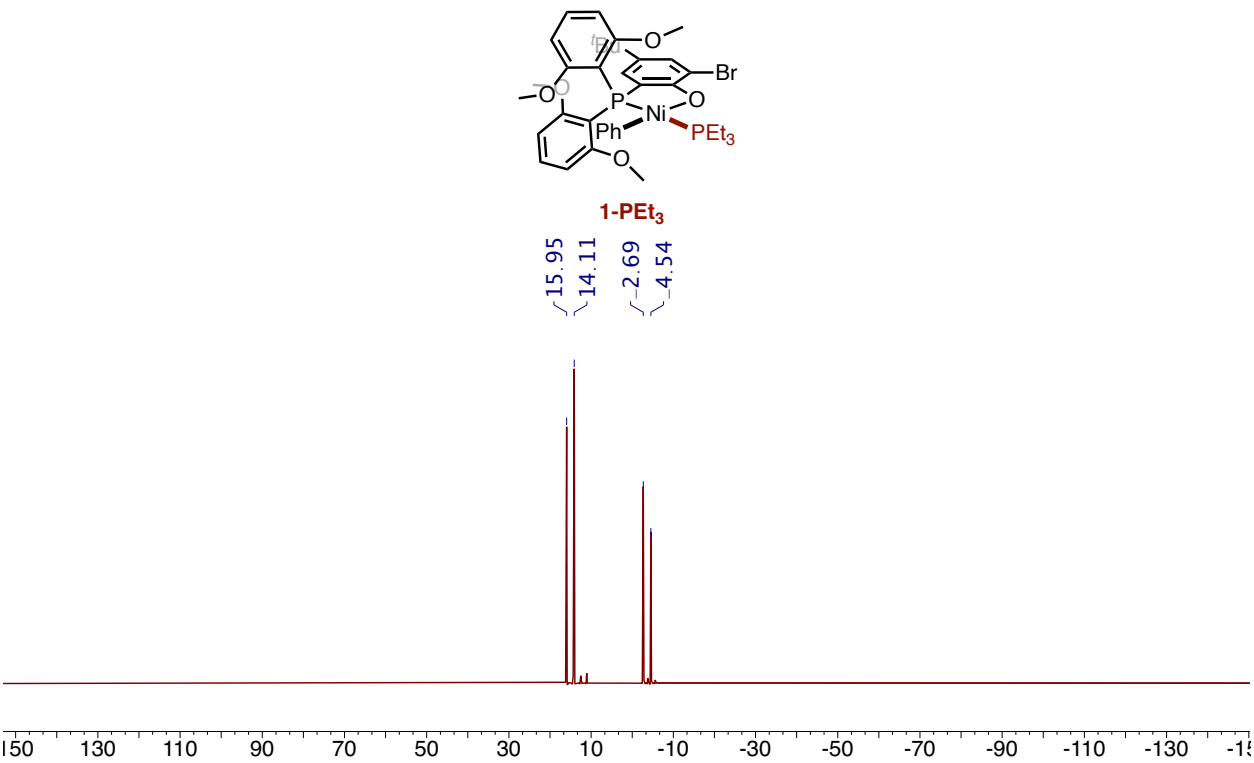

Figure S19. $^{31}P\{^{1}H\}$ NMR spectrum of **1-PEt$_3$** in C_6D_6.

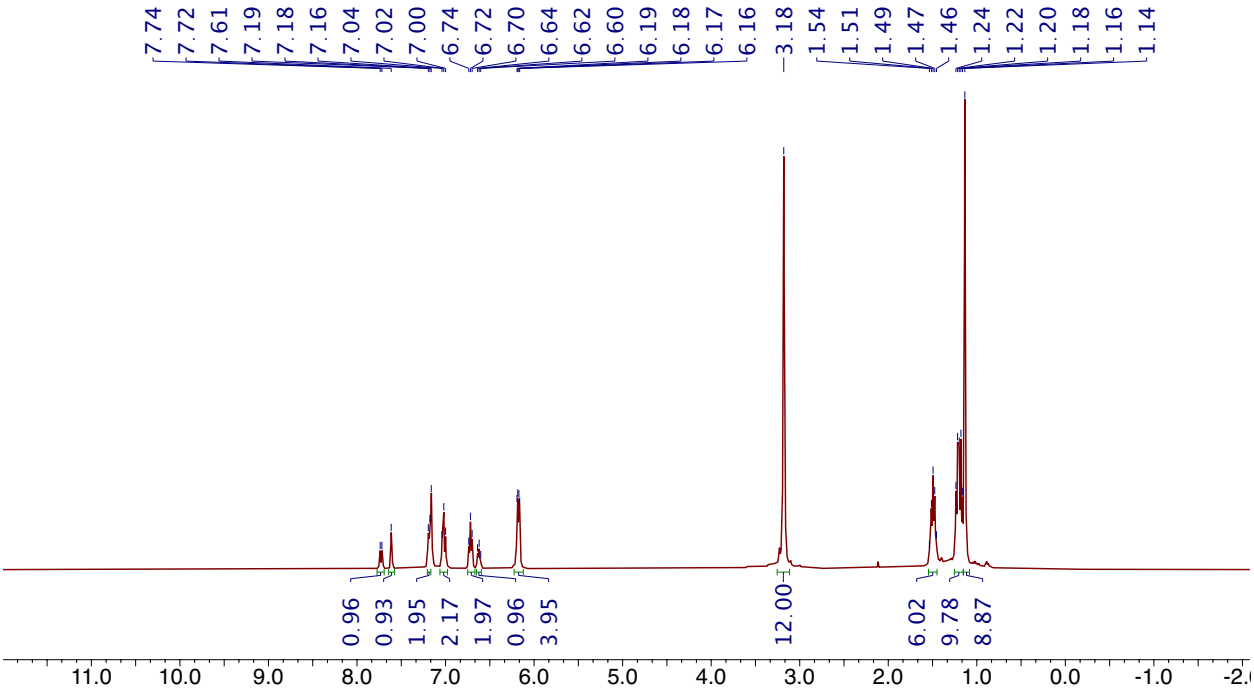

Figure S20. ^{1}H NMR spectrum of **1-PEt$_3$** in C_6D_6.

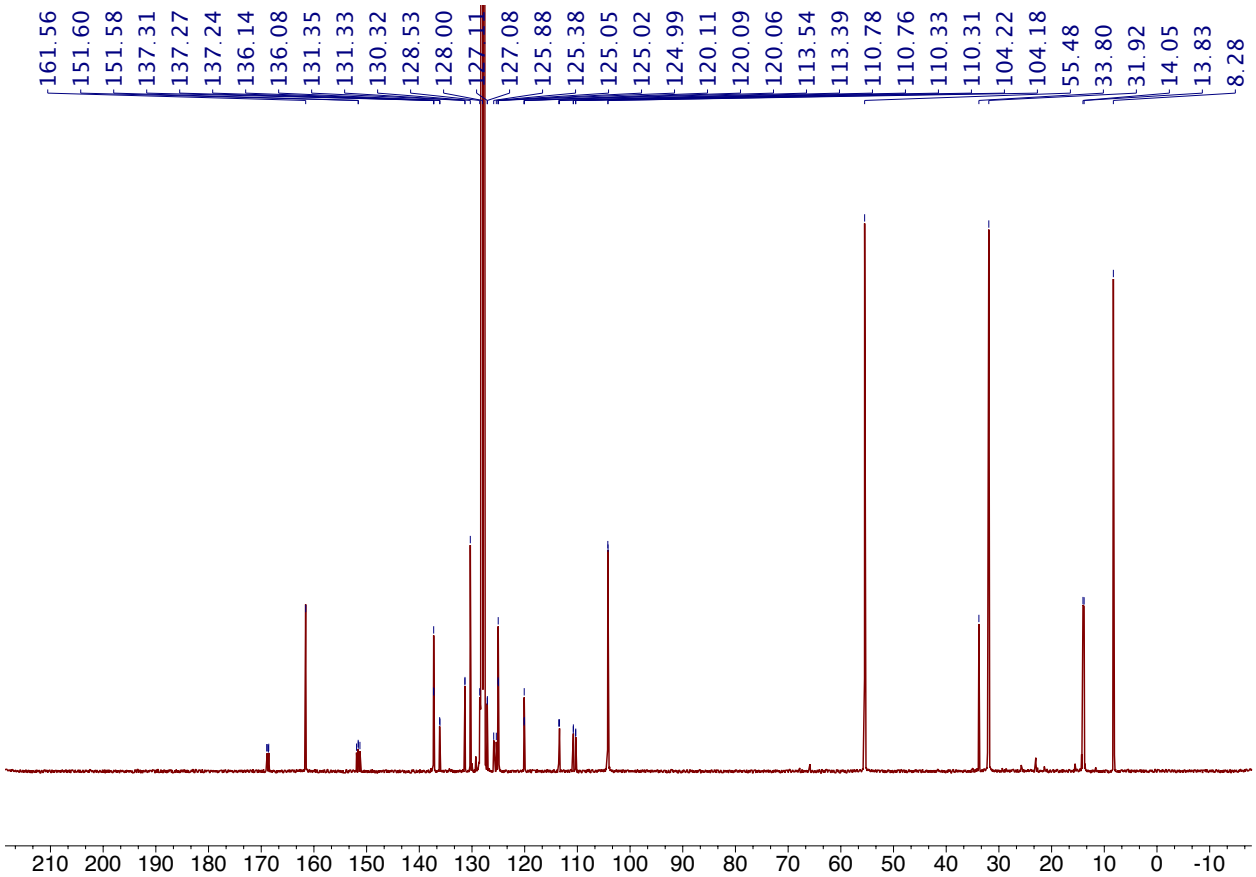

Figure S21. $^{13}C\{^{1}H\}$ NMR spectrum of **1-PEt$_3$** in C_6D_6.

5. Crystallographic Information

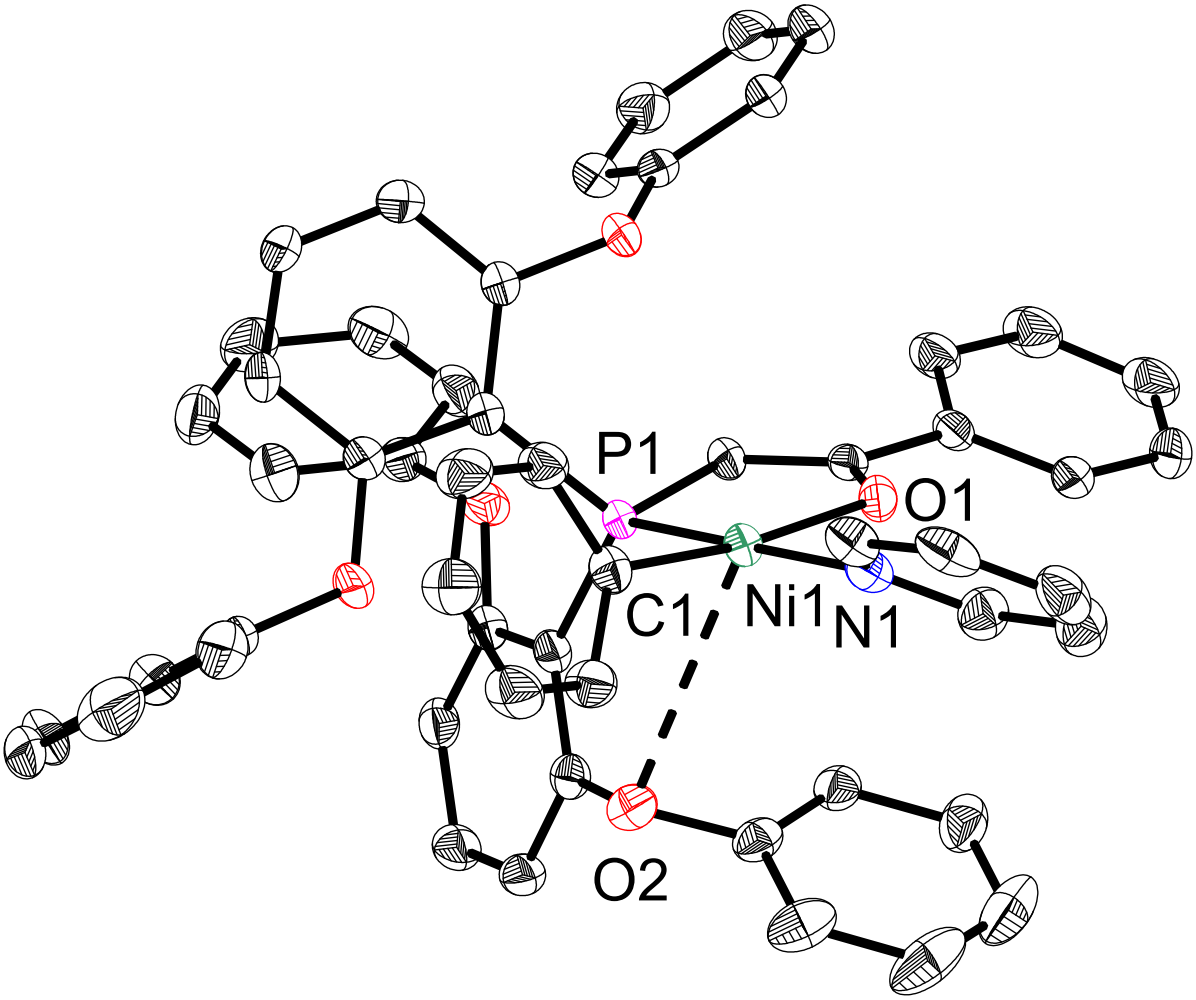

Figure S22. Solid-State Structure of **2-py**. Ellipsoids are shown at the 50% probability level. Hydrogen atoms and solvent molecules excluded for clarity.

Special Refinement Details for 2-py: Complex **2-py** crystalizes as needles/needle-like thin blocks in a P-1 space group with two molecules in the asymmetric unit (only one is shown in figure S22 for clarity), as well as one outer-sphere diethyl ether molecule.

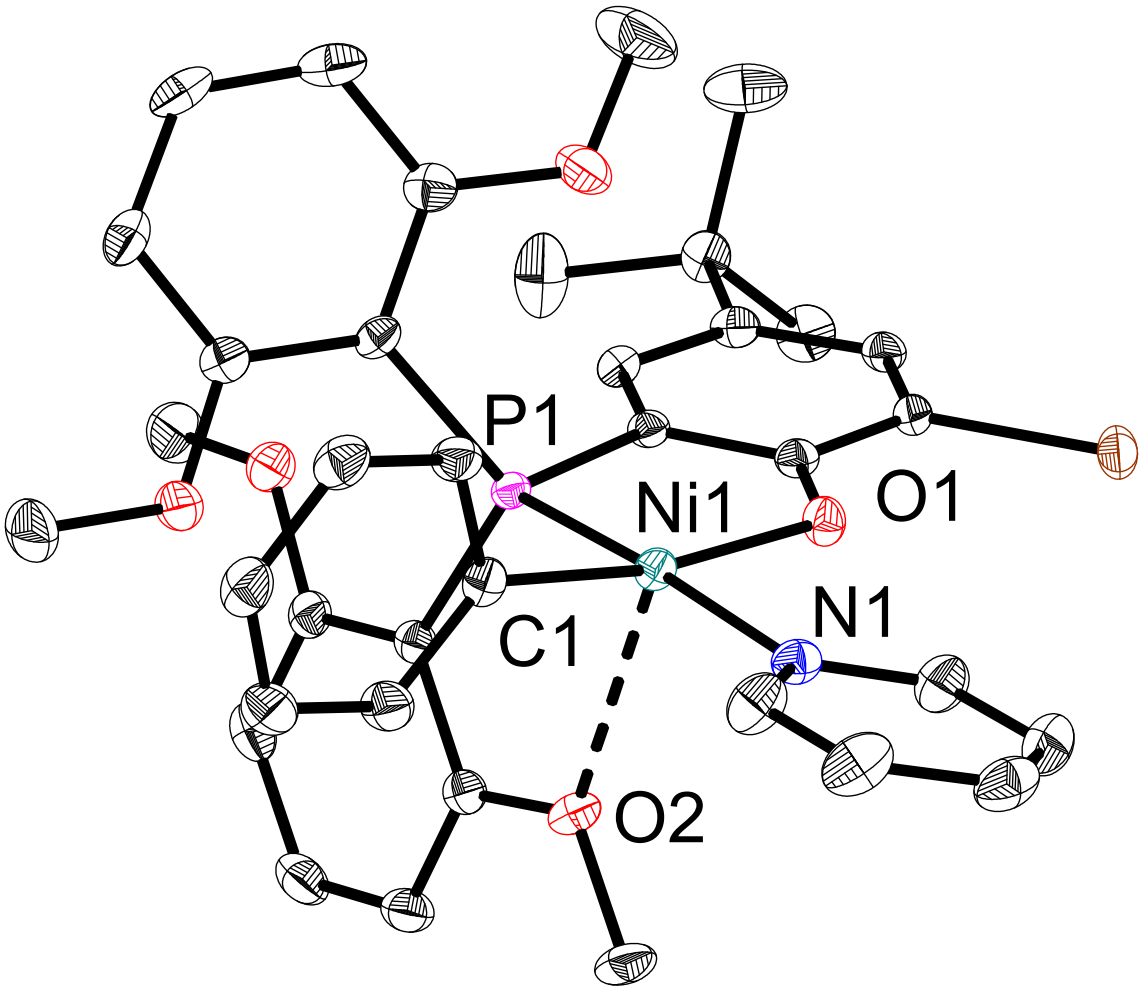

Figure S23. Solid-State Structure of **1-py**. Ellipsoids are shown at the 50% probability level. Hydrogen atoms and solvent molecules excluded for clarity.

Special Refinement Details for 1-py: Complex **1-py** crystalizes in a P-1 space group with one molecule in the asymmetric unit.

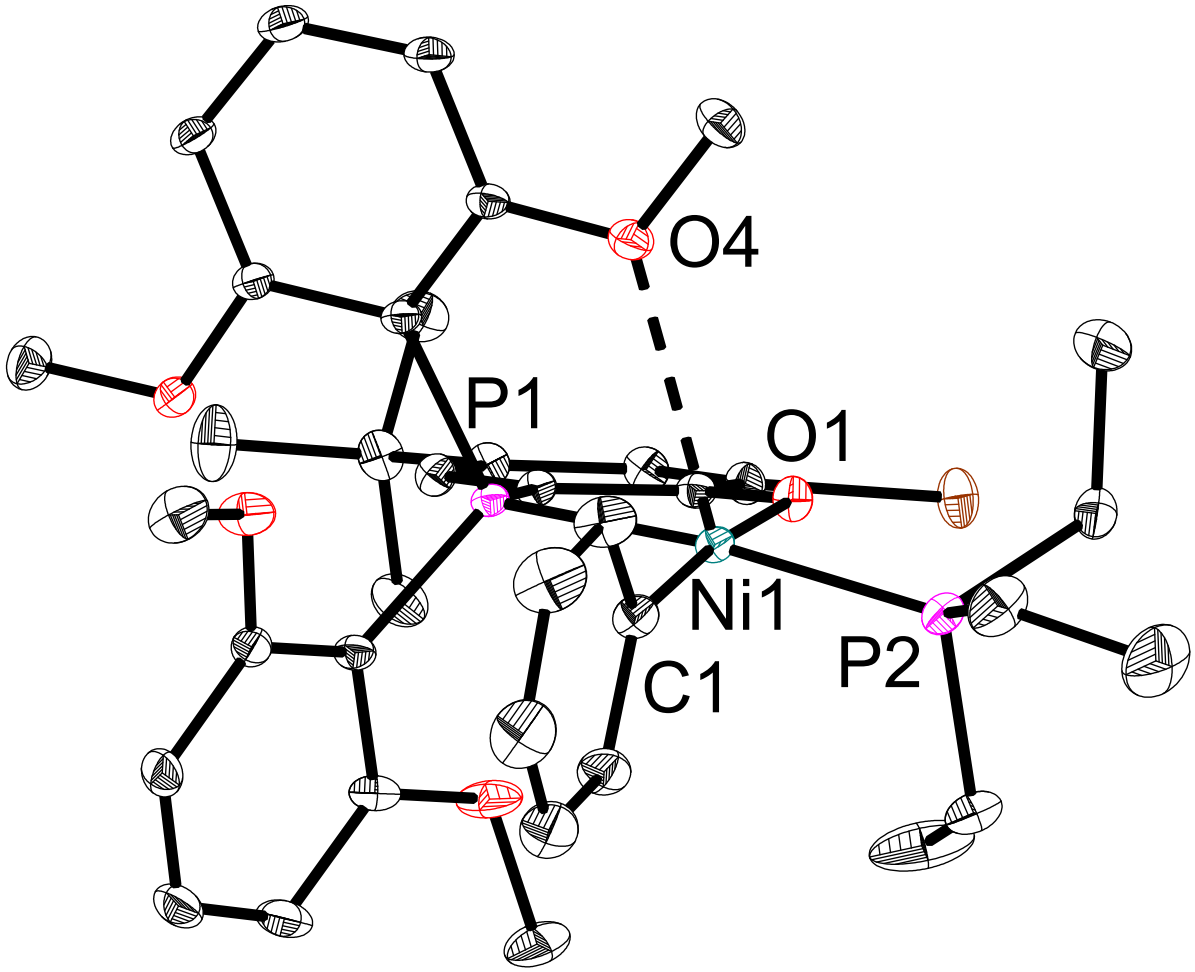

Figure S24. Solid-State Structure of **1-PEt$_3$**. Ellipsoids are shown at the 50% probability level. Hydrogen atoms and solvent molecules excluded for clarity.

Special Refinement Details for 1-PEt$_3$: Complex **1-PEt$_3$** crystalizes in a P-1 space group with one molecule in the asymmetric unit.

Crystallographic Information

Table S1. Crystal and refinement data.

	1-PEt$_3$	**1-py**	**2-py**
CCDC	2240825	2240827	2240826
Empirical formula	$C_{38}H_{49}BrNiO_5P_2$	$C_{37}H_{39}BrNNiO_5P$	$C_{57}H_{47}NNiO_{5.5}P$
Formula weight	786.3	747.3	923.6
Temperature/K	100	100.0	100
Crystal system	Triclinic	Monoclinic	Triclinic
Space group	P-1	$P2_1/n$	P-1
a/Å	10.3124(4)	11.6704(12)	12.607(1)
b/Å	13.674(3)	20.7729(18)	17.131(1)
c/Å	14.277(3)	14.1219(11)	23.826(1)
α/°	98.571(11)	90	90.931(2)
β/°	100.819(12)	95.872(8)	91.839(2)
γ/°	103.599(13)	90	99.079(2)
Volume/Å^3	1882.2(7)	3405.6(5)	5077.2(4)
Z	2	4	4
ϱ_{calc}g/cm^3	1.388	1.458	1.208
μ/mm^{-1}	1.702	2.993	1.232
F(000)	821	1535	1932
Radiation	MoKα (λ = 0.71073)	CuKα (λ = 1/54178)	CuKα (λ = 1/54178)
Reflections collected	89011	11904	118128
Independent reflections	20596	6520	19869
Goodness-of-fit on F^2	1.018	1.033	1.049
Final R indexes [I>=2σ (I)]	R_1 = 2.90 %, R_2 = 7.17 %	R_1 = 3.06 %, R_2 = 7.94 %	R_1 = 6.24 %, R_2 = 19.19 %

6. Procedures for Polymerization and Polymer characterization

6.1 General procedure for high throughput parallel polymerization reactor (PPR) runs for preparation of polyethylene and ethylene/tBA copolymers.

Polyolefin catalysis screening was performed in a high throughput parallel polymerization reactor (PPR) system. The PPR system was comprised of an array of 48 single cell (6 x 8 matrix) reactors in an inert atmosphere glovebox. Each cell was equipped with a glass insert with an internal working liquid volume of approximately 5 mL. Each cell had independent controls for pressure and was continuously stirred at 800 rpm. Catalyst solutions (with $Ni(COD)_2$ if necessary) were prepared in toluene. All liquids (i.e., solvent, tBA, and catalyst solutions) were added via robotic syringes. Gaseous reagents (i.e., ethylene) were added via a gas injection port. Prior to each run, the reactors were heated to 50 °C, purged with ethylene, and vented.

All desired cells were injected with tBA followed with a portion of toluene (This step was skipped for ethylene homopolymerization). The reactors were heated to the run temperature and then pressured to the appropriate psig with ethylene. Catalyst solutions (with $Ni(COD)_2$ if necessary) were then added to the cells. Each catalyst addition was chased with a small amount of toluene so that after the final addition, a total reaction volume of 5 mL was reached. Upon addition of the catalyst, the PPR software began monitoring the pressure of each cell. The desired pressure (within approximately 2-6 psig) was maintained by the supplemental addition of ethylene gas by opening the valve at the set point minus 1 psi and closing it when the pressure reached 2 psi higher. All drops in pressure were cumulatively recorded as "Uptake" or "Conversion" of the ethylene for the duration of the run or until the uptake or conversion requested value was reached, whichever occurred first. Each reaction was then quenched by addition of 1% oxygen in nitrogen for 30 seconds at 40 psi higher than the reactor pressure. The pressure of each cell was monitored during and after the quench to ensure that no further ethylene consumption happens. The shorter the "Quench Time" (the duration between catalyst addition and oxygen quench), the more active the catalyst. In order to prevent the formation of too much polymer in any given cell, the reaction was quenched upon reaching a predetermined uptake level of 80 psig. After all the reactors were quenched,

they were allowed to cool to about 60 °C. They were then vented, and the tubes were removed. The polymer samples were then dried in a centrifugal evaporator at 60 °C for 12 hours, weighed to determine polymer yield and used in subsequent IR (tBA incorporation), GPC (molecular weight), DSC (melting temperature) and NMR (copolymer microstructures) analysis.

6.1.1 Measurement of ethylene uptake curves

Upon addition of the catalyst, the PPR software began monitoring the pressure of each cell. The desired pressure (within approximately 2-6 psig) was maintained by the supplemental addition of ethylene gas by opening the valve at the set point minus 1 psi and closing it when the pressure reached 2 psi higher. For example, the pressure was maintained between approximately 399-402 psi if the original pressure was set to 400 psi. All drops in pressure were cumulatively recorded as "Uptake" or "Conversion" of the ethylene for the duration of the run**.** The unit of this "Uptake" is in psi and the uptake curves over time were used to analyze the real-time activity of catalysts and rates of chain propagation.

6.2 General procedure for batch reactor runs for preparation of ethylene/tBA copolymers.

Polymerization reactions were conducted in a 2-L Parr batch reactor. The reactor was heated by an electrical heating mantle and cooled by an internal serpentine cooling coil containing cooling water. The water was pre-treated by passing through an Evoqua water purification system. Both the reactor and the heating/cooling system were controlled and monitored by a Camile TG process computer. The bottom of the reactor was fitted with a dump valve, which empties the reactor contents into a lidded dump pot, which was prefilled with a catalyst-kill solution (typically 5 mL of an Irgafos / Irganox / toluene mixture). The lidded dump pot was vented to a 15-gal. blowdown tank, with both the pot and the tank N_2 purged. All chemicals used for polymerization or catalyst makeup are run through purification columns to remove any impurities that may affect polymerization. The toluene was passed through two columns, the first containing A2 alumina, the second containing Q5 reactant. The tert-butyl acrylate was filtered through activated alumina. The ethylene was passed through two columns, the first containing A204 alumina and 4 Å molecular sieves, the second containing Q5 reactant. The N2 used for transfers was passed through a single column containing A204 alumina, 4 Å molecular sieves and Q5 reactant.

The reactor was loaded first from the shot tank that contained toluene and tBA. The shot tank was filled to the load set points by use of a differential pressure transducer. After solvent/acrylate addition, the shot tank was rinsed twice with toluene. Then the reactor was heated up to the polymerization temperature set point. The ethylene was added to the reactor when the reaction temperature was reached to maintain the reaction pressure set point. Ethylene addition amounts were monitored by a micro-motion flowmeter.

The catalysts were handled in an inert atmosphere glovebox and were prepared as a solution in toluene. The catalyst was drawn into a syringe and pressure-transferred into the catalyst shot tank. This was followed by 3 rinses of toluene, 5 mL each. Catalyst was added when the reactor pressure set point was reached.

Immediately after catalyst addition the run timer was started. Usually within the first 2 min. of successful catalyst runs an exotherm was observed, as well as decreasing reactor pressure. Ethylene was then added by the Camile to maintain reaction pressure set point in the reactor. These polymerizations were run until 40 g of ethylene uptake. Then the agitator was stopped, and the bottom dump valve was opened to empty reactor contents into the lidded dump pot. The lidded dump pot was closed and the contents were poured into trays placed in a lab hood where the solvent was evaporated off overnight. The trays containing the remaining polymer were then transferred to a vacuum oven, where they were heated up to 140 °C under vacuum to remove any remaining solvent. After the trays cooled to ambient temperature, the polymers were weighed for yield/efficiencies and submitted for polymer testing if so desired.

6.3 General procedure for polymer characterization

6.3.1 Gel permeation chromatography (GPC)

High temperature GPC analysis was performed using a Dow Robot Assisted Delivery (RAD) system equipped with a Polymer Char infrared detector (IR5) and Agilent PLgel Mixed A columns. Decane (10 μL) was added to each sample for use as an internal flow marker. Samples were first diluted in 1,2,4-trichlorobenzene (TCB) stabilized with 300 ppm butylated hydroxyl toluene (BHT) at a concentration of

10 mg/mL and dissolved by stirring at 160°C for 120 minutes. Prior to injection the samples are further diluted with TCB stabilized with BHT to a concentration of 3 mg/mL. Samples (250 μL) are eluted through one PL-gel 20 μm (50 x 7.5 mm) guard column followed by two PL-gel 20 μm (300 x 7.5 mm) Mixed-A columns maintained at 160 °C with TCB stabilized with BHT at a flowrate of 1.0 mL/min. The total run time was 24 minutes. To calibrate for molecular weight (MW) Agilent EasiCal polystyrene standards (PS-1 and PS-2) were diluted with 1.5 mL TCB stabilized with BHT and dissolved by stirring at 160 °C for 15 minutes. These standards are analyzed to create a 3rd order MW calibration curve. Molecular weight units are converted from polystyrene (PS) to polyethylene (PE) using a daily Q-factor calculated to be around 0.4 using the average of 5 Dowlex 2045 reference samples.

6.3.2 Fourier-transform infrared spectroscopy (FTIR)

The 10 mg/mL samples prepared for GPC analysis are also utilized to quantify tert-butyl acrylate (tBA) incorporation by Fourier Transform infrared spectroscopy (FTIR). A Dow robotic preparation station heated and stirred the samples at 160°C for 60 minutes then deposited 130 μL portions into stainless wells promoted on a silicon wafer. The TCB was evaporated off at 160°C under nitrogen purge. IR spectra were collected using a Nexus 6700 FT-IR equipped with a DTGS KBr detector from 4000-400 cm-1 utilizing 128 scans with a resolution of 4. Ratio of tBA (C=O: 1762-1704 cm−1) to ethylene (CH2: 736-709 cm−1) peak areas were calculated and fit to a linear calibration curve to determine total tBA.

6.3.3 Differential scanning calorimetry (DSC)

Differential scanning calorimetry analyses was performed on solid polymer samples using a TA Instruments, Inc. Discovery Series or TA Instruments, Inc., DSC2500, programmed with the following method:

Equilibrate at 175.00 °C

Isothermal for 3 minutes

Ramp 30.00 °C/min to 0.00 °C

Ramp 10.00 °C/min to 175.00 °C

Data was analyzed using TA Trios software.

6.3.4 NMR characterization

NMR spectra of ethylene/tBA copolymers were recorded on a Bruker 400 MHz using o-dichlorobenzene at 120 °C. ^{1}H NMR analysis of copolymers were done using a relaxation time (0.2 s), and an acquisition time (1.8 s) with the number of FID's collected per sample (512). $^{13}C\{^{1}H\}$ NMR analysis of copolymers were done using 90° pulse of 17.2 μs, a relaxation time (22.0 s), an acquisition time (5.3 s), and inverse-gated decoupling with the number of FID's collected per sample (1024). Analysis of the spectra was based on literature.[5-6]

7. Supplemental Data for Ethylene/tBA Copolymerization

7.1 Supplemental ethylene uptake curves

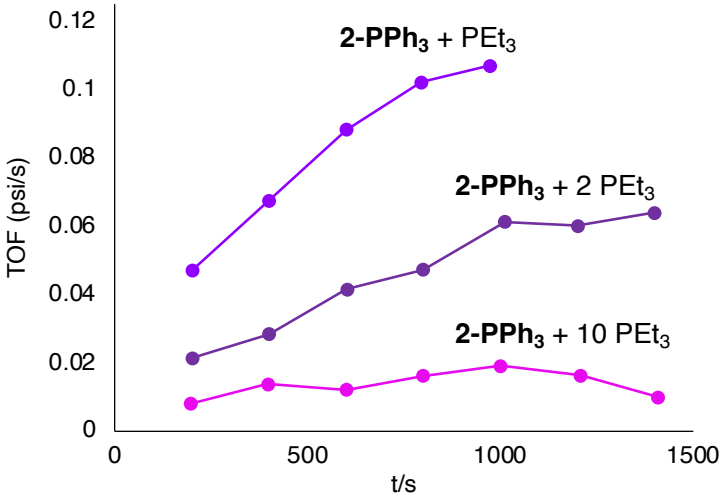

Figure S25. Rate of ethylene uptake (TOF) vs time with different PEt_3 concentrations (Catalyst: **2-PPh$_3$**). Condition: V = 5 mL, [Ni] = 0.05 mM, ethylene pressure = 400 psi, [tBA] = 0.05 M, toluene solvent. See Table S6 for original catalytic runs.

7.2 Original catalytic runs of ethylene/tBA copolymerization included in Table 1

Table S2. Original data for table 1.

Entry[a]	Catalyst	[Ni]/mM	[tBA]/M	T/°C	t/s	Isolated Yield/mg	Activity[b]	$M_w/10^3$	PDI	%Mol tBA	Tm/°C
1	**1-PEt$_3$**	0.05	0.05	90	3601	47	190	60.27	2.22	1.79	113
2	**1-PEt$_3$**	0.05	0.05	90	3600	54	220	65.20	2.38	1.67	114
3	**1-PEt$_3$**	0.05	0.05	90	3601	57	230	63.92	2.21	1.66	114
4	**1-PEt$_3$**	0.05	0.1	90	3600	31	120	39.75	2.25	3.47	104
5	**1-PEt$_3$**	0.05	0.1	90	3600	31	120	42.83	2.95	3.48	103
6	**1-py**	0.05	0.05	90	1761	125	1020	79.63	2.24	1.66	115
7	**1-py**	0.05	0.05	90	1457	114	1130	76.73	2.58	1.61	115
8	**1-py**	0.05	0.05	90	1504	122	1170	78.96	2.13	1.47	N.D.
9	**1-py**	0.05	0.1	90	3601	104	420	54.16	2.17	3.25	105
10	**1-py**	0.05	0.1	90	3600	118	470	55.79	2.17	3.23	105
11	**2-PEt$_3$**	0.05	0.05	90	1304	117	1300	10.34	2.27	0.50	122
12	**2-PEt$_3$**	0.05	0.05	90	1125	113	1400	10.14	2.41	0.55	122
13	**2-PEt$_3$**	0.05	0.05	90	1213	115	1400	10.62	2.41	0.54	122
14	**2-PEt$_3$**	0.05	0.05	90	1274	124	1400	10.06	2.20	0.53	122
15	**2-py**	0.05	0.05	90	296	114	5500	10.32	2.32	0.57	122
16	**2-py**	0.05	0.05	90	280	123	6300	11.04	2.84	0.56	121
17	**2-py**	0.05	0.05	90	252	118	6800	9.16	2.76	0.56	121

18	**2-py**	0.05	0.05	90	323	141	6300	10.66	2.25	0.52	122
19	**2-PPh$_3$**	0.05	0.05	90	342	128	5400	11.95	2.13	0.51	121
20	**2-PPh$_3$**	0.05	0.05	90	320	126	5700	13.12	1.92	N.D.	124
21	**2-PPh$_3$**	0.05	0.05	90	304	124	5900	11.38	2.18	0.50	121
22	**2-PPh$_3$** + 1 PEt$_3$	0.05	0.05	90	973	126	1860	11.24	2.20	0.50	120
23	**2-PPh$_3$** + 1 PEt$_4$	0.05	0.05	90	1096	140	1840	10.06	2.24	0.53	122
24	**2-PPh$_3$** + 1 PEt$_5$	0.05	0.05	90	865	115	1910	11.96	1.94	0.45	122
25	**2-PPh$_3$** + 2 PEt$_3$	0.05	0.05	90	1545	119	1110	10.27	2.34	0.51	122
26	**2-PPh$_3$** + 2 PEt$_4$	0.05	0.05	90	1268	108	1230	9.86	2.38	0.51	122
27	**2-PPh$_3$** + 2 PEt$_5$	0.05	0.05	90	1309	114	1250	10.57	2.61	0.50	122
28	**2-PPh$_3$** + 10 PEt$_6$	0.05	0.05	90	3601	40	160	3.16	2.22	0.47	121
29	**2-PPh$_3$** + 10 PEt$_7$	0.05	0.05	90	3601	46	190	3.57	2.21	0.46	121
30	**2-PPh$_3$** + 10 PEt$_8$	0.05	0.05	90	3600	47	190	4.50	2.82	0.48	121
31	**2-PEt$_3$**	0.05	0.05	110	493	126	3700	8.55	2.48	0.66	120
32	**2-PEt$_3$**	0.05	0.05	110	454	113	3600	7.84	2.45	0.58	122
33	**2-PEt$_3$**	0.05	0.05	110	417	111	3800	8.10	2.34	0.49	121
34	**2-py**	0.05	0.05	110	169	142	12100	6.63	2.43	0.70	123
35	**2-py**	0.05	0.05	110	159	143	12900	6.70	2.55	0.66	122
36	**2-py**	0.05	0.05	110	145	150	14900	7.17	2.18	0.52	122
37	**2-py**	0.05	0.1	110	399	135	4900	7.40	2.60	1.11	113
38	**2-py**	0.05	0.1	110	368	121	4700	6.74	2.34	1.14	115
39	**2-py**	0.05	0.1	110	376	120	4600	6.17	2.48	1.20	113
40	**2-py**	0.05	0.15	110	587	117	2900	6.68	2.43	1.51	113
41	**2-py**	0.05	0.15	110	571	118	3000	6.48	2.24	1.60	111
42	**2-PEt$_3$**	0.025	0.025	90	587	117	3400	11.43	2.37	0.33	125
43	**2-PEt$_3$**	0.025	0.025	90	571	118	2600	11.13	2.29	0.32	125
44	**2-py**	0.025	0.025	90	323	130	11600	14.09	3.37	0.31	125
45	**2-py**	0.025	0.025	90	302	120	11400	12.03	2.43	0.30	123
46	**2-py**	0.025	0.025	90	323	131	11700	12.38	2.15	0.29	123
47	**2-py**	0.025	0.025	90	209	143	19700	11.66	2.54	0.24	126
48	**2-PEt$_3$**	0.025	0.025	110	492	120	7000	14.09	3.37	0.31	125
49	**2-PEt$_3$**	0.025	0.025	110	470	122	7500	12.03	2.43	0.30	123
50	**2-PEt$_3$**	0.025	0.025	110	455	116	7300	12.38	2.15	0.29	123
51	**2-PEt$_3$**	0.025	0.025	110	452	119	7600	11.66	2.54	0.24	126
52	**2-py**	0.025	0.025	110	186	138	21000	8.56	2.42	0.32	124
53	**2-py**	0.025	0.025	110	180	144	23000	7.72	2.53	0.32	124
54	**2-py**	0.025	0.025	110	162	135	24000	7.96	2.56	0.33	124
55	**2-py**	0.025	0.025	110	139	136	28000	8.27	2.36	0.29	123

[a]Unless specified, V = 5 mL, [Ni] = 0.05 mM, ethylene pressure = 400 psi, toluene solvent; polymerization was stopped after consuming a set amount of ethylene. [b]Activity in kg/(mol·h).

7.2 Original ethylene/tBA copolymerization runs of ethylene uptake curves.

Table S3. Original ethylene/tBA copolymerization runs of ethylene uptake curves included in Figure 2a

Entry[a]	Catalyst	[Ni]/mM	[tBA]/M	T/°C	t/s	Isolated Yield/mg	Activity[b]	$M_w/10^3$	PDI	%Mol tBA	Tm/°C
1	**2-PEt$_3$**	0.025	0.025	110	470	122	7500	12.03	2.43	0.3	123
2	**2-py**	0.025	0.025	110	162	135	24000	7.96	2.56	0.33	124

[a]Unless specified, V = 5 mL, ethylene pressure = 400 psi, toluene solvent; polymerization was stopped after consuming a set amount of ethylene. Entries 1~2 were also included in table S2 as entry 49, and 54, respectively. [b]Activity in kg/(mol·h).

Table S4. Original ethylene/tBA copolymerization runs of ethylene uptake curves included in Figure 2b-c

Entry[a]	Catalyst	[Ni(COD)$_2$]/mM	[tBA]/M	T/°C	t/s	Isolated Yield/mg	Activity[b]	$M_w/10^3$	PDI	%Mol tBA	Tm/°C
1	**1-PEt$_3$**	0.05	0.05	90	3601	57	230	63.92	2.21	1.66	114
2	**1-py**	0.05	0.05	90	1504	122	1170	78.96	2.13	1.47	N.D.
3[c]	**2-py**	0	0.05	110	159	143	12900	6.7	2.55	0.66	122
4	**2-py**	0	0.10	110	376	120	4600	6.17	2.48	1.2	110
5	**2-py**	0	0.15	110	571	118	3000	6.48	2.24	1.6	111
6	**2-py**	0	0.05	90	323	141	6300	10.66	2.25	0.52	122
7	**2-PEt$_3$**	0	0.05	90	1053	101	1380	10.6	2.40	0.5	122
8[d]	**2-PEt$_3$**	0.20	0.05	90	743	100	2000	10.3	2.70	0.6	122

[a]Unless specified, V = 5 mL, [Ni] = 0.05 mM, ethylene pressure = 400 psi, toluene solvent; polymerization was stopped after consuming a set amount of ethylene. Entries 1~4 were also included in table S2 as entry 35, 39, 41, and 16, respectively. [b]Activity in kg/(mol·h). [c]Reported in ref 3 (Table S6.3, entry 37). [d]Reported in ref 3 (Table S6.3, entry 24).

Table S5. Original ethylene/tBA copolymerization runs of ethylene uptake curves included in Figure 3

Entry[a]	Catalyst	[Ni(COD)$_2$]/mM	[tBA]/M	T/°C	t/s	Isolated Yield/mg	Activity[b]	$M_w/10^3$	PDI	%Mol tBA	Tm/°C
1[c]	**^{Me}PO^{Ph}-Ni(P)**	0	0.05	90	3600	51	210	2.9	2.1	2.0	114
2	**2-PEt$_3$**	0	0.05	90	1053	101	1380	10.6	2.4	0.5	122
3	**^{Ph}PO^{PhCF3}-Ni(P)**	0	0.05	90	1156	106	1320	6.3	2.2	0.5	122
4	**^{Ph}PO^{ArOMe}-Ni(P)**	0	0.05	90	1148	116	1460	11.5	2.5	0.6	121
5[d]	**^{Ph}P*O^{ArO}-Ni(P)**	0	0.05	90	3412	94	400	10.2	2.5	0.6	122

[a]Unless specified, V = 5 mL, [Ni] = 0.05 mM, ethylene pressure = 400 psi, toluene solvent; polymerization was stopped after consuming a set amount of ethylene. [b]Activity in kg/(mol·h). [c]Reported in ref 3 (Table S6.3, entry 37). [d]Reported in ref 3 (Table S6.3, entry 24).

Table S6. Original ethylene/tBA copolymerization runs of ethylene uptake curves included in Figure S25

Entry[a]	Catalyst	T/°C	t/s	Isolated Yield/mg	Activity[b]	$M_w/10^3$	PDI	%Mol tBA	Tm/°C
1	**2-PPh$_3$** + 1 PEt$_3$	90	973	126	1860	11.24	2.20	0.50	120
2	**2-PPh$_3$** + 2 PEt$_3$	90	1545	119	1110	10.27	2.34	0.51	122
3	**2-PPh$_3$** + 10 PEt$_6$	90	3601	40	160	3.16	2.22	0.47	121

[a]Unless specified, V = 5 mL, [Ni] = 0.05 mM, ethylene pressure = 400 psi, [tBA] = 0.05 M, toluene solvent; polymerization was stopped after consuming a set amount of ethylene. Entries 1~3 were also included in table S2 as entry 22, 25, 28, and 16, respectively. [b]Activity in kg/(mol·h).

8. Characterization of ethylene/tBA copolymers

8.1 Samples of ^{1}H and $^{13}C\{^{1}H\}$ spectra of ethylene/tBA copolymers

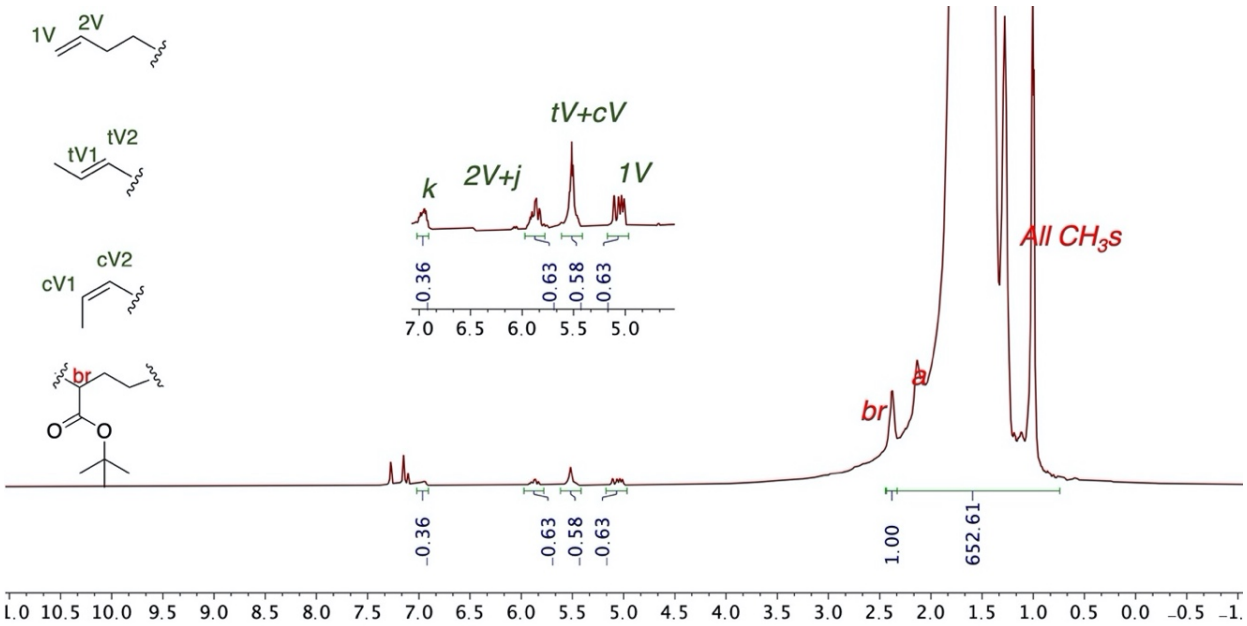

Figure S26. ^{1}H NMR spectrum of ethylene/tBA copolymer **P*** (Table S2, entry 15).

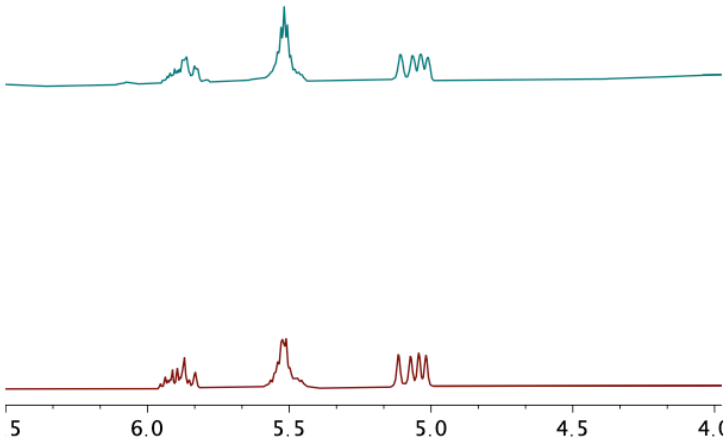

Figure S27. Comparison of ^{1}H NMR spectra of ethylene/tBA copolymer **P*** (top) and **P** (bottom) (Note: Copolymer samples **P** is the copolymers produced by **2-PEt$_3$** and has been reported in ref 2b as sample C. Sample P and P* were produced in ethylene/tBA copolymerization by **2-PEt$_3$** or **2-py** under otherwise identical conditions.)

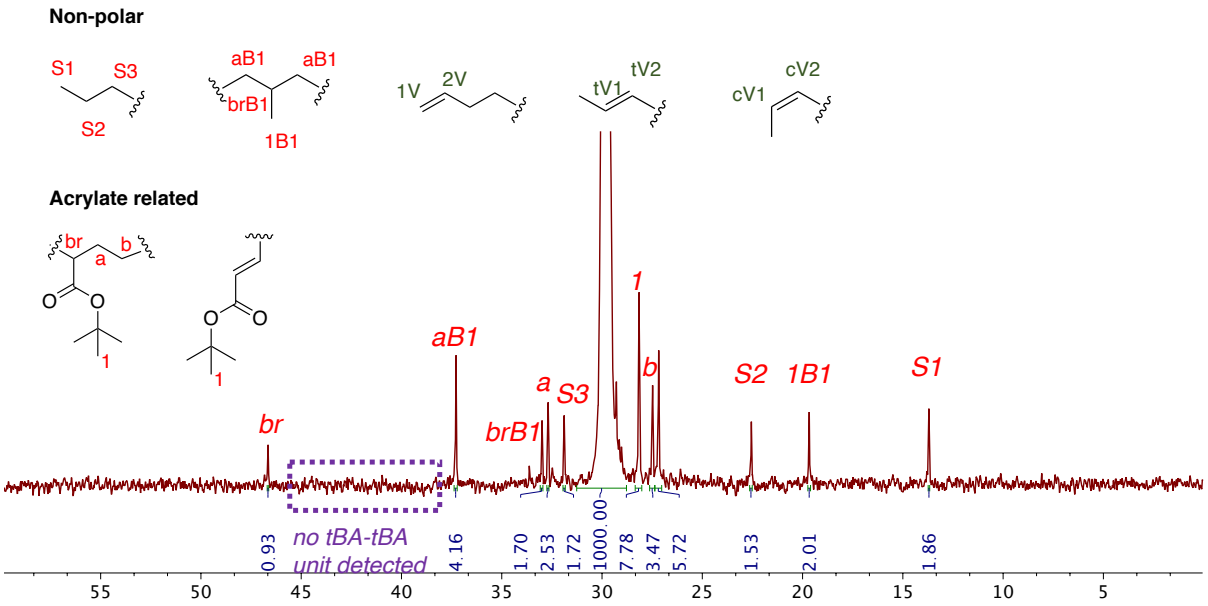

Figure S28. $^{13}C\{^{1}H\}$ NMR spectrum of ethylene/tBA copolymer **P*** with peaks assigned to specific microstructural features.

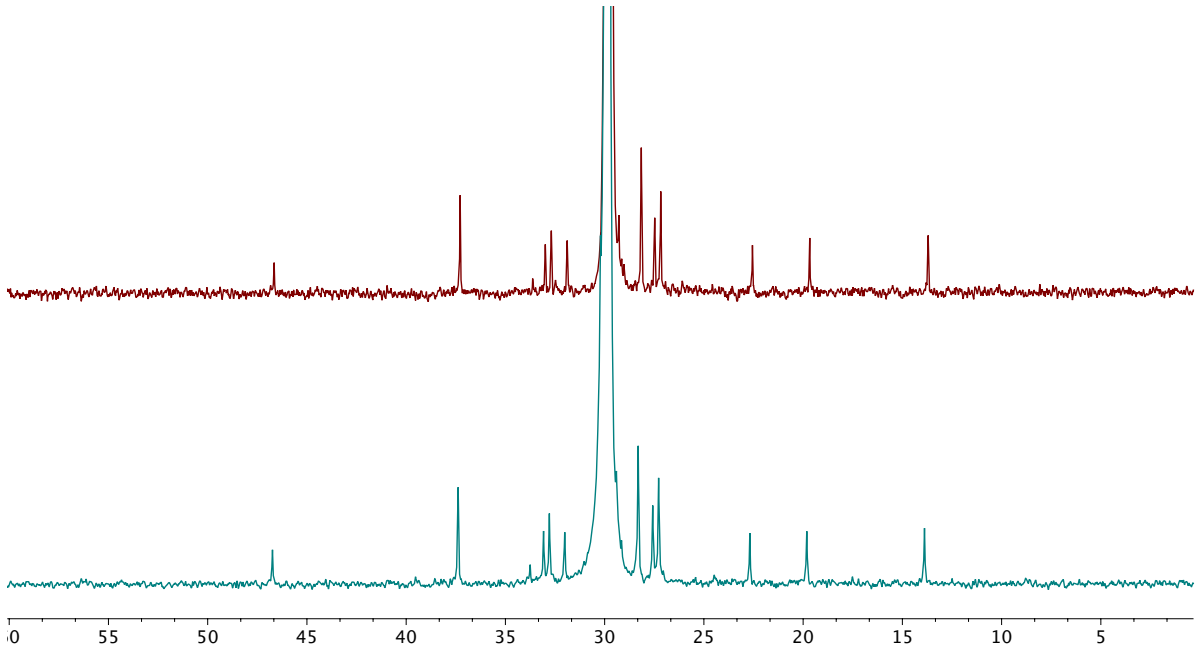

Figure S29. Comparison of $^{13}C\{^{1}H\}$ NMR spectra of ethylene/tBA copolymer **P*** (top) and **P** (bottom)

8.2 Microstructural analysis

8.2.1 Calculation of Mn based on ^{1}H NMR spectra

Below shown the calculation of Mn from a ^{1}H NMR spectrum (Figure S25). Note that the integration of the resonance of *br* set to 1, therefore all values of integration in ^{1}H NMR spectra are all relevant numbers of protons per occurrence of a tBA units (labeled as rX)

rX = relevant number of carbon atoms

rX-H = relevant number of proton atoms = 652.63 + 0. 63 + 0.58 + 0.63 + 0.36 = 654.83

Each ethylene unit has 2 carbon and 4 protons

For tBA units, each tBA unit has 6 carbon and 12 protons exclude the ester group (-C(O)O-). Note that the relevant number of tBA units is 1 (reference).

Therefore **rX = 0.5 * rX-H + 1**

rC = relevant number of polymer chain

rC = 0.5 * 0.63 + 0.5 * 0.58 + 0.36 = 0.965

M_n = (rX * 12 + rX-H * 1 + 2 * Mol Wt (O))/rC = ((0.5 * rX-H + 1) * 12 + rX-H + 2 * 16)/rC = (7 * 654.83 + 6 + 32)/0.965 = 4.789k ~ 4.8k

For comparison, the molecular weight obtained by GPC is M_n =4.45 k

8.2.2 Methods of microstructural analysis

- **%Mol tBA (NMR)**

Calculation of % Mol tBA (NMR) is based on the ^{1}H NMR spectrum and section S7.1.2.

rR = relevant number of repeating units = 0.5 * (rX-4) = 0.25 * rX-H - 1.5

Relevant number of tBA units = 1

% Mol tBA = 1 / rR = 1 / (0.25 * rX-H - 1.5)

For sample **P***, % Mol tBA = 1 / (0.25 * 654.83 - 1.5) = 0.6 %, which is consistent with the result obtained from quantitative FTIR.

- **%I-tBA**

%I-tBA is the percentage of internal tBA units over all tBA units. Calculation of **%I-tBA** is based on the $^{13}C\{^{1}H\}$ NMR spectrum. Note that all tBA units have t-butyl group (peak 1) but only internal tBA units have saturated α- and β-carbon (peak a, b). For sample **P***:

% I -tBA = (0.5 * Integration of peak b)/(0.333 * Integration of peak 1) = 67%

- **%T-tBA**

%T-tBA is the percentage of terminal tBA units over all tBA units.

%T-tBA = 1 - %I-tBA

For sample **P***, **%T-tBA** = 33%

- **%Vinyl**

% Vinyl is the ratio of the number of terminal vinyl units over the number of tBA units in percentage.

% Vinyl is calculated based on the ^{1}H NMR spectra and section S7.1.2. For sample **P***:

rV = relevant number of vinyls = 0.5 * integration of peak 1V

rT-tBA = relevant number of terminal tBA = integration of peak k (if cis-end tBA is not present)

%Vinyl/%T-tBA=rV/rT-tBA

For sample **P***, % Vinyl = 29%

- **N(Methyl)**

Calculation of **N(Methyl)** is based on the $^{13}C\{^{1}H\}$ NMR spectrum (unit: 1/1000C).

N(Methyl) = 1000 * Integration of 1B1/Intergration of all main-chain carbons

For sample **P***, **N(Methyl)** = 2.0

- **N(2-Propenyl)**

Calculation of **N(2-Propenyl)** is based on the ^{1}H NMR spectrum (unit: 1/1000C).

N(2-Propenyl) = 1000 * relevant number of propenyl/rX = 1000 * (0.5 * integration of peak (TV+CV)/(0.5 * rX-H + 1)

For sample **P***, **N(2-Propenyl)** = 0.9

8.2.3 Comparison of copolymer microstructures

Copolymer samples **P** is the copolymers produced by **2-PEt$_3$** (reported in ref 2b as sample C). Sample P and P* were produced in ethylene/tBA copolymerization by **2-PEt$_3$** or **2-py** under otherwise identical conditions.

Table S7 Comparison of ethylene/tBA copolymers **P** and **P***.

	P	**P***
Catalyst	**2-PEt$_3$**	**2-py**
Mn(GPC)/10^3	4.36	4.45
% I-tBA	59%	67%
% T-tBA	41%	33%
% Vinyl	21%	29%
Methyl/1000C	1.7	2.0
2-Propenyl/1000C	0.6	0.9
Mn(NMR)/10^3	4.76	4.78

8.3 A samples of GPC curves of ethylene/tBA copolymers

Conventional GPC & Composition Results

LIMS #:	22-0604	Description:	*Library 385457 Vial 19*
Project:		Report by:	
For:	FileProc	Method:	Not Selected

MWD Results: Conventional GPC	
Mn	4,450
Mp	8,990
Mv	9,410
Mw	10,320
Mz	18,640
PDI	2.32

Quadrant Analysis		
25%	21270	
50%	10300	10
75%	5800	
100%	2150	
Whole	7160	
50% Ratio	3.97	-60
		271.64

Run Parameters:	
Conc	2.0000
Inj. Vol.	250.0
Mass Inj.	0.5000
MassRec.	88.50%
System Parameters:	
Flow Rate	1.0010
Flow Marker	18.501
Ref Flow Marker	18.482
Rec. Flow Rate	

Comonomer Type	Octene
Avg SCB/1000TC	9.61
Avg Wt% Comonomer	9.24
Avg Corrected Wt%	7.69

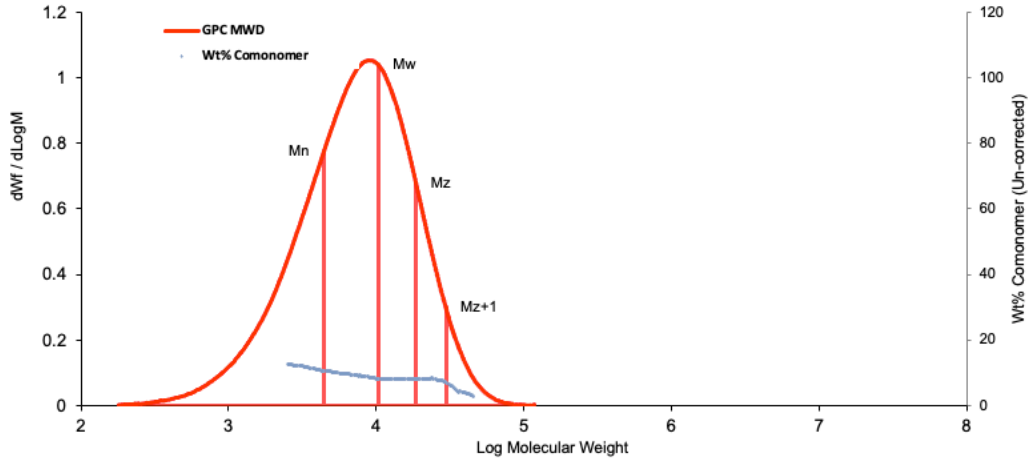

Figure S30. GPC curve of ethylene/tBA copolymers (table S2, entry 15).

8.4 A sample of DSC curves of ethylene/tBA copolymers

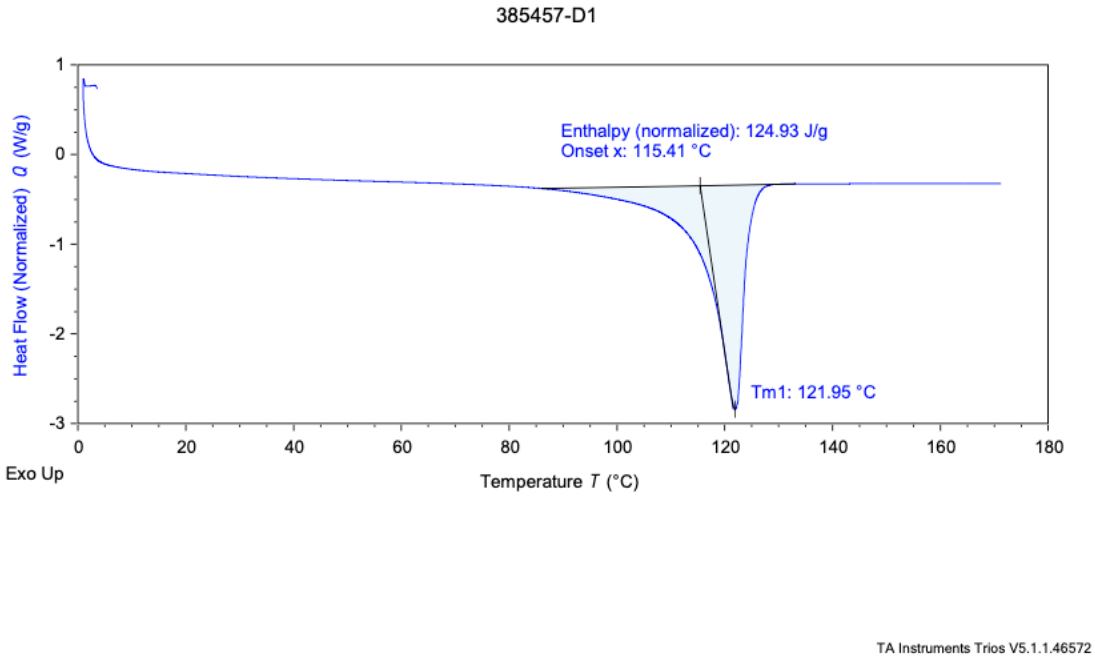

Figure S31. GPC curve of ethylene/tBA copolymers (table S2, entry 15).

9. Catalyst comparison

The catalysts reported here are notable for high activity and thermal stability for polar polyolefin synthesis. A variety of catalysts have been developed for ethylene/acrylate copolymerization.[5-76] Previous examples of nickel catalyzed ethylene acrylate copolymerization are relatively rare, with the majority supported by phenoxide/napthoxide-based ligands. [5-6, 10-11, 13, 16, 73, 77] To compare the performance of our best catalyst, **2-py** to prior examples, two metrics were plotted: catalyst activity and tBA incorporation (Figure S31).

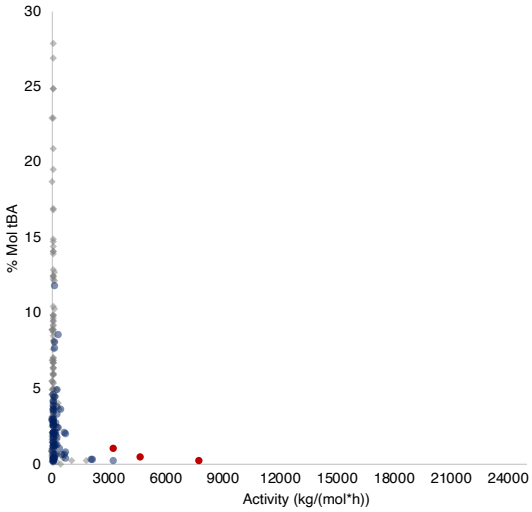

Figure S32. Reported Pd and Ni catalysts for ethylene/acrylate copolymerization (diamonds: palladium examples; circles: nickel examples; red circles: **2-PEt$_3$**; darker color indicates overlapping data points; reported catalysts are included if they: 1) show activity higher than 0.5 kg/(mol*h) in ethylene acrylate copolymerization and 2) produce copolymers with M_w>2500).

Previously reported ethylene/acrylate copolymerization experiments were included if they feature: 1) activity > 0.5 kg/(mol*h) and 2) copolymer M_w >2500. In addition, experiments are excluded if they were performed with large amounts of activator/masking reagents on a scale comparable to the amount of acrylate (additives:acrylates > 1:10). Overall, experiments under 468 different reaction conditions, or 229 different catalysts, from 75 scientific papers are included in catalyst comparison.[5-76] Reaction conditions, such the ethylene pressure, catalyst and monomer concentration, may differ, therefore these comparisons should be considered qualitative.

Overall, most examples show limited activities of less than 100 kg/(mol·h) (423 out of 468 experiments, or 200 out of 229 catalysts), though being able to produce copolymers with varying molecular weights, branching distribution and polar monomer incorporation. An important aspect to consider is that increased acrylate incorporation will result in lower activity, which affects some of the systems compared. Specifically, both catalyst activity and tBA incorporation are limited for Ni-catalyzed ethylene/acrylate copolymerization, except a recent example showing ability to incorporate up to 12 mol% tBA.[6] **2-PEt$_3$**, a catalyst we recently reported, displays significant improved activity (yellow data points) compared to previous reports.

The best catalyst included in this work, **2-py**, displays further improvements in activity (Figure S32)

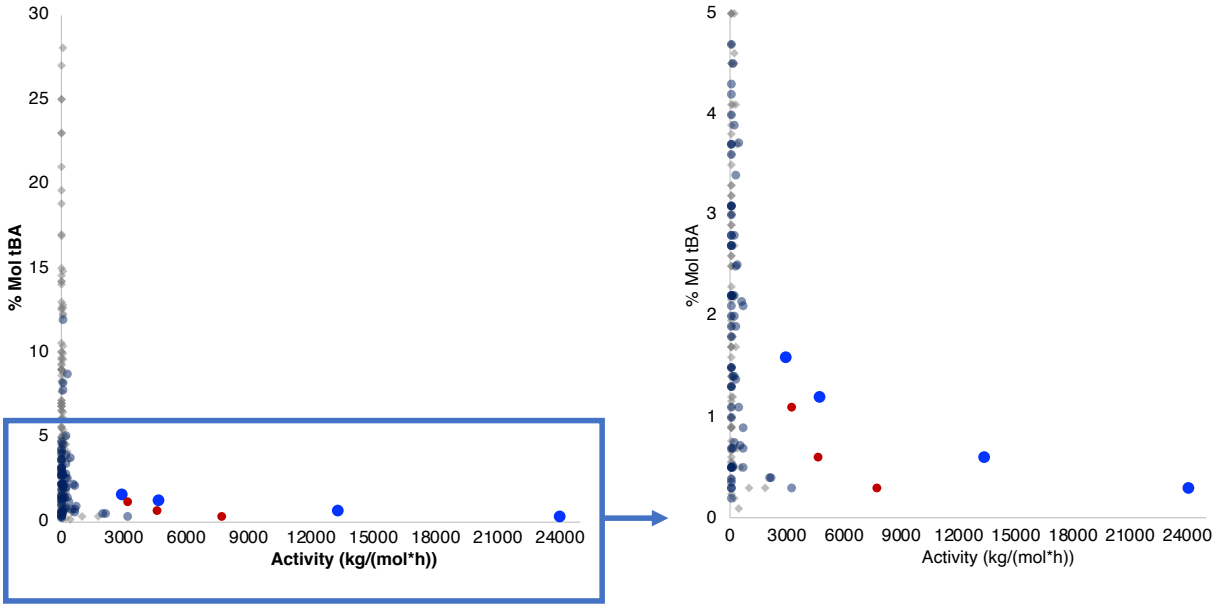

Figure S33. Comparison of **2-py** with reported Pd and Ni catalysts for ethylene/acrylate copolymerization (diamonds: palladium examples; circles: nickel examples, red circles: **2-PEt$_3$**; blue circles: **2-py**; darker color indicates overlapping data points; reported catalysts are included if they: 1) show activity higher than 0.5 kg/(mol*h) in ethylene acrylate copolymerization and 2) produce copolymers with M_w >2500).

References

(1) Waltman, A. W.; Younkin, T. R.; Grubbs, R. H., Insights into the deactivation of neutral nickel ethylene polymerization catalysts in the presence of functionalized olefins. *Organometallics* **2004,** *23* (22), 5121-5123.

(2) Marshall, W. J.; Grushin, V. V., Activation of chlorobenzene with Ni(0) N,N-chelates — A remarkably profound effect of a minuscule change in ligand structure. *Canadian Journal of Chemistry* **2005,** *83* (6-7), 640-645.

(3) Xiong, S.; Hong, A.; Bailey, B. C.; Spinney, H. A.; Senecal, T. D.; Bailey, H.; Agapie, T., Highly Active and Thermally Robust Nickel Enolate Catalysts for the Synthesis of Ethylene-Acrylate Copolymers. *Angew. Chem. Int. Ed.* **2022**.

(4) Guironnet, D.; Roesle, P.; Rünzi, T.; Göttker-Schnetmann, I.; Mecking, S., Insertion polymerization of acrylate. *J. Am. Chem. Soc.* **2009,** *131* (2), 422-423.

(5) Xin, B. S.; Sato, N.; Tanna, A.; Oishi, Y.; Konishi, Y.; Shimizu, F., Nickel catalyzed copolymerization of ethylene and alkyl acrylates. *J. Am. Chem. Soc.* **2017,** *139* (10), 3611-3614.

(6) Xiong, S.; Shoshani, M. M.; Zhang, X.; Spinney, H. A.; Nett, A. J.; Henderson, B. S.; Miller III, T. F.; Agapie, T., Efficient Copolymerization of Acrylate and Ethylene with Neutral P, O-Chelated Nickel Catalysts: Mechanistic Investigations of Monomer Insertion and Chelate Formation. *J. Am. Chem. Soc.* **2021,** *143* (17), 6516-6527.

(7) Johnson, L. K.; Mecking, S.; Brookhart, M., Copolymerization of ethylene and propylene with functionalized vinyl monomers by palladium (II) catalysts. *J. Am. Chem. Soc.* **1996,** *118* (1), 267-268.

(8) Nakano, R.; Nozaki, K., Copolymerization of propylene and polar monomers using Pd/IzQO catalysts. *J. Am. Chem. Soc.* **2015,** *137* (34), 10934-10937.

(9) Takano, S.; Takeuchi, D.; Osakada, K.; Akamatsu, N.; Shishido, A., Dipalladium catalyst for olefin polymerization: Introduction of acrylate units into the main chain of branched polyethylene. *Angew. Chem. Int. Ed.* **2014,** *53* (35), 9246-9250.

(10) Zhang, Y.; Mu, H.; Wang, X.; Pan, L.; Li, Y., Elaborate tuning in ligand makes a big difference in catalytic performance: bulky nickel catalysts for (co) polymerization of ethylene with promising vinyl polar monomers. *ChemCatChem* **2019,** *11* (9), 2329-2340.

(11) Chen, M.; Chen, C., A Versatile Ligand Platform for Palladium-and Nickel-Catalyzed Ethylene Copolymerization with Polar Monomers. *Angew. Chem. Int. Ed.* **2018,** *57* (12), 3094-3098.

(12) Saki, Z.; D'Auria, I.; Dall'Anese, A.; Milani, B.; Pellecchia, C., Copolymerization of Ethylene and Methyl Acrylate by Pyridylimino Ni (II) Catalysts Affording Hyperbranched Poly (ethylene-co-methyl acrylate) s with Tunable Structures of the Ester Groups. *Macromolecules* **2020,** *53* (21), 9294-9305.

(13) Tahmouresilerd, B.; Xiao, D.; Do, L. H., Rigidifying Cation-Tunable Nickel Catalysts Increases Activity and Polar Monomer Incorporation in Ethylene and Methyl Acrylate Copolymerization. *Inorg. Chem.* **2021**.

(14) Tao, W. j.; Nakano, R.; Ito, S.; Nozaki, K., Copolymerization of ethylene and polar monomers by using Ni/IzQO catalysts. *Angew. Chem. Int. Ed.* **2016,** *55* (8), 2835-2839.

(15) Li, M.; Wang, X.; Luo, Y.; Chen, C., A Second-Coordination-Sphere Strategy to Modulate Nickel-and Palladium-Catalyzed Olefin Polymerization and Copolymerization. *Angew. Chem. Int. Ed.* **2017,** *56* (38), 11604-11609.

(16) Zhang, Y.; Mu, H.; Pan, L.; Wang, X.; Li, Y., Robust bulky [P, O] neutral nickel catalysts for copolymerization of ethylene with polar vinyl monomers. *ACS Catal.* **2018,** *8* (7), 5963-5976.

(17) Ye, J.; Mu, H.; Wang, Z.; Jian, Z., Heteroaryl backbone strategy in bisphosphine monoxide palladium-catalyzed ethylene polymerization and copolymerization with polar monomers. *Organometallics* **2019,** *38* (15), 2990-2997.
(18) Cui, L.; Jian, Z., A N-bridged strategy enables hemilabile phosphine–carbonyl palladium and nickel catalysts to mediate ethylene polymerization and copolymerization with polar vinyl monomers. *Polym. Chem* **2020,** *11* (38), 6187-6193.
(19) Zou, C.; Liao, D.; Pang, W.; Chen, M.; Tan, C., Versatile PNPO ligands for palladium and nickel catalyzed ethylene polymerization and copolymerization with polar monomers. *J. Catal.* **2021,** *393*, 281-289.
(20) Drent, E.; van Dijk, R.; van Ginkel, R.; van Oort, B.; Pugh, R. I., Palladium catalysed copolymerisation of ethene with alkylacrylates: polar comonomer built into the linear polymer chain. *Chem. Commun.* **2002,** (7), 744-745.
(21) Jenkins, J. C.; Brookhart, M., A mechanistic investigation of the polymerization of ethylene catalyzed by neutral Ni (II) complexes derived from bulky anilinotropone ligands. *J. Am. Chem. Soc.* **2004,** *126* (18), 5827-5842.
(22) Popeney, C. S.; Camacho, D. H.; Guan, Z., Efficient incorporation of polar comonomers in copolymerizations with ethylene using a cyclophane-based Pd (II) α-diimine catalyst. *J. Am. Chem. Soc.* **2007,** *129* (33), 10062-10063.
(23) Neuwald, B.; Olscher, F.; Göttker-Schnetmann, I.; Mecking, S., Limits of activity: weakly coordinating ligands in arylphosphinesulfonato palladium (II) polymerization catalysts. *Organometallics* **2012,** *31* (8), 3128-3137.
(24) Piche, L.; Daigle, J. C.; Rehse, G.; Claverie, J. P., Structure–Activity Relationship of Palladium Phosphanesulfonates: Toward Highly Active Palladium-Based Polymerization Catalysts. *Chem. - Eur. J.* **2012,** *18* (11), 3277-3285.
(25) Wucher, P.; Goldbach, V.; Mecking, S., Electronic influences in phosphinesulfonato palladium (II) polymerization catalysts. *Organometallics* **2013,** *32* (16), 4516-4522.
(26) Jian, Z.; Wucher, P.; Mecking, S., Heterocycle-substituted phosphinesulfonato palladium (II) complexes for insertion copolymerization of methyl acrylate. *Organometallics* **2014,** *33* (11), 2879-2888.
(27) Ota, Y.; Ito, S.; Kuroda, J.-i.; Okumura, Y.; Nozaki, K., Quantification of the steric influence of alkylphosphine–sulfonate ligands on polymerization, leading to high-molecular-weight copolymers of ethylene and polar monomers. *J. Am. Chem. Soc.* **2014,** *136* (34), 11898-11901.
(28) Pan, H.; Zhu, L.; Li, J.; Zang, D.; Fu, Z.; Fan, Z., A thermal stable α-diimine palladium catalyst for copolymerization of ethylene with functionalized olefins. *Journal of Molecular Catalysis A: Chemical* **2014,** *390*, 76-82.
(29) Zhu, L.; Fu, Z.-S.; Pan, H.-J.; Feng, W.; Chen, C.; Fan, Z.-Q., Synthesis and application of binuclear α-diimine nickel/palladium catalysts with a conjugated backbone. *Dalton Trans* **2014,** *43* (7), 2900-2906.
(30) Allen, K. E.; Campos, J. s.; Daugulis, O.; Brookhart, M., Living polymerization of ethylene and copolymerization of ethylene/methyl acrylate using "sandwich" diimine palladium catalysts. *ACS Catal.* **2015,** *5* (1), 456-464.
(31) Chen, M.; Yang, B.; Chen, C., Redox-Controlled Olefin (Co) Polymerization Catalyzed by Ferrocene-Bridged Phosphine-Sulfonate Palladium Complexes. *Angew. Chem. Int. Ed.* **2015,** *54* (51), 15520-15524.

(32) Dai, S.; Sui, X.; Chen, C., Highly Robust Palladium (II) α-Diimine Catalysts for Slow-Chain-Walking Polymerization of Ethylene and Copolymerization with Methyl Acrylate. *Angew. Chem. Int. Ed.* **2015,** *54* (34), 9948-9953.
(33) Dai, S.; Chen, C., Direct synthesis of functionalized high-molecular-weight polyethylene by copolymerization of ethylene with polar monomers. *Angew. Chem. Int. Ed.* **2016,** *55* (42), 13281-13285.
(34) Hu, H.; Chen, D.; Gao, H.; Zhong, L.; Wu, Q., Amine–imine palladium catalysts for living polymerization of ethylene and copolymerization of ethylene with methyl acrylate: incorporation of acrylate units into the main chain and branch end. *Polym. Chem* **2016,** *7* (3), 529-537.
(35) Mitsushige, Y.; Carrow, B. P.; Ito, S.; Nozaki, K., Ligand-controlled insertion regioselectivity accelerates copolymerisation of ethylene with methyl acrylate by cationic bisphosphine monoxide–palladium catalysts. *Chem. Sci.* **2016,** *7* (1), 737-744.
(36) Wang, R.; Zhao, M.; Chen, C., Influence of ligand second coordination sphere effects on the olefin (co) polymerization properties of α-diimine Pd (II) catalysts. *Polym. Chem* **2016,** *7* (23), 3933-3938.
(37) Wu, Z.; Chen, M.; Chen, C., Ethylene polymerization and copolymerization by palladium and nickel catalysts containing naphthalene-bridged phosphine–sulfonate ligands. *Organometallics* **2016,** *35* (10), 1472-1479.
(38) Zou, W.; Chen, C., Influence of backbone substituents on the ethylene (co) polymerization properties of α-diimine Pd (II) and Ni (II) catalysts. *Organometallics* **2016,** *35* (11), 1794-1801.
(39) Liang, T.; Chen, C., Side-arm control in phosphine-sulfonate palladium-and nickel-catalyzed ethylene polymerization and copolymerization. *Organometallics* **2017,** *36* (12), 2338-2344.
(40) Sui, X.; Hong, C.; Pang, W.; Chen, C., Unsymmetrical α-diimine palladium catalysts and their properties in olefin (co) polymerization. *Mater. Chem. Front.* **2017,** *1* (5), 967-972.
(41) Tao, W.; Akita, S.; Nakano, R.; Ito, S.; Hoshimoto, Y.; Ogoshi, S.; Nozaki, K., Copolymerisation of ethylene with polar monomers by using palladium catalysts bearing an N-heterocyclic carbene–phosphine oxide bidentate ligand. *Chem. Commun.* **2017,** *53* (17), 2630-2633.
(42) Wu, Z.; Hong, C.; Du, H.; Pang, W.; Chen, C., Influence of ligand backbone structure and connectivity on the properties of phosphine-sulfonate Pd (II)/Ni (II) catalysts. *Polymers* **2017,** *9* (5), 168.
(43) Yang, B.; Xiong, S.; Chen, C., Manipulation of polymer branching density in phosphine-sulfonate palladium and nickel catalyzed ethylene polymerization. *Polym. Chem* **2017,** *8* (40), 6272-6276.
(44) Zhai, F.; Solomon, J. B.; Jordan, R. F., Copolymerization of ethylene with acrylate monomers by amide-functionalized α-diimine Pd catalysts. *Organometallics* **2017,** *36* (9), 1873-1879.
(45) Zhang, D.; Chen, C., Influence of Polyethylene Glycol Unit on Palladium-and Nickel-Catalyzed Ethylene Polymerization and Copolymerization. *Angew. Chem. Int. Ed.* **2017,** *56* (46), 14672-14676.
(46) Zhao, M.; Chen, C., Accessing multiple catalytically active states in redox-controlled olefin polymerization. *ACS Catal.* **2017,** *7* (11), 7490-7494.
(47) Zhong, S.; Tan, Y.; Zhong, L.; Gao, J.; Liao, H.; Jiang, L.; Gao, H.; Wu, Q., Precision synthesis of ethylene and polar monomer copolymers by palladium-catalyzed living coordination copolymerization. *Macromolecules* **2017,** *50* (15), 5661-5669.
(48) Cai, Z.; Do, L. H., Thermally Robust Heterobimetallic Palladium–Alkali Catalysts for Ethylene and Alkyl Acrylate Copolymerization. *Organometallics* **2018,** *37* (21), 3874-3882.

(49) Ding, L.; Cheng, H.; Li, Y.; Tanaka, R.; Shiono, T.; Cai, Z., Efficient ethylene copolymerization with polar monomers using palladium anilinonaphthoquinone catalysts. *Polym. Chem* **2018,** *9* (45), 5476-5482.
(50) Guo, L.; Liu, Y.; Sun, W.; Du, Q.; Yang, Y.; Kong, W.; Liu, Z.; Chen, D., Synthesis, characterization, and olefin (co) polymerization behavior of unsymmetrical α-diimine palladium complexes containing bulky substituents at 4-position of aniline moieties. *J. Organomet. Chem.* **2018,** *877*, 12-20.
(51) Zhang, W.; Waddell, P. M.; Tiedemann, M. A.; Padilla, C. E.; Mei, J.; Chen, L.; Carrow, B. P., Electron-rich metal cations enable synthesis of high molecular weight, linear functional polyethylenes. *J. Am. Chem. Soc.* **2018,** *140* (28), 8841-8850.
(52) Du, C.; Zhong, L.; Gao, J.; Zhong, S.; Liao, H.; Gao, H.; Wu, Q., Living (co) polymerization of ethylene and bio-based furfuryl acrylate using dibenzobarrelene derived α-diimine palladium catalysts. *Polym. Chem* **2019,** *10* (16), 2029-2038.
(53) Liao, Y.; Zhang, Y.; Cui, L.; Mu, H.; Jian, Z., Pentiptycenyl substituents in insertion polymerization with α-diimine nickel and palladium species. *Organometallics* **2019,** *38* (9), 2075-2083.
(54) Li, K.; Ye, J.; Wang, Z.; Mu, H.; Jian, Z., Indole-bridged bisphosphine-monoxide palladium catalysts for ethylene polymerization and copolymerization with polar monomers. *Polym. Chem* **2020**.
(55) Li, S.; Dai, S., 8-Arylnaphthyl substituent retarding chain transfer in insertion polymerization with unsymmetrical α-diimine systems. *Polym. Chem* **2020,** *11* (45), 7199-7206.
(56) Park, D.-A.; Byun, S.; Ryu, J. Y.; Lee, J.; Lee, J.; Hong, S., Abnormal N-Heterocyclic Carbene–Palladium Complexes for the Copolymerization of Ethylene and Polar Monomers. *ACS Catal.* **2020,** *10* (10), 5443-5453.
(57) Tan, C.; Qasim, M.; Pang, W.; Chen, C., Ligand–metal secondary interactions in phosphine–sulfonate palladium and nickel catalyzed ethylene (co) polymerization. *Polym. Chem* **2020,** *11* (2), 411-416.
(58) Xu, M.; Yu, F.; Li, P.; Xu, G.; Zhang, S.; Wang, F., Enhancing chain initiation efficiency in the cationic allyl-nickel catalyzed (co) polymerization of ethylene and methyl acrylate. *Inorg. Chem.* **2020,** *59* (7), 4475-4482.
(59) Zhang, Y.; Wang, C.; Mecking, S.; Jian, Z., Ultrahigh branching of main-chain-functionalized polyethylenes by inverted insertion selectivity. *Angew. Chem.* **2020,** *132* (34), 14402-14408.
(60) Zhong, L.; Zheng, H.; Du, C.; Du, W.; Liao, G.; Cheung, C. S.; Gao, H., Thermally robust α-diimine nickel and palladium catalysts with constrained space for ethylene (co) polymerizations. *J. Catal.* **2020,** *384*, 208-217.
(61) Zhou, G.; Mu, H.; Jian, Z., A comprehensive picture on catalyst structure construction in palladium catalyzed ethylene (co) polymerizations. *J. Catal.* **2020,** *383*, 215-220.
(62) Akita, S.; Nozaki, K., Copolymerization of ethylene and methyl acrylate by palladium catalysts bearing IzQO ligands containing methoxyethyl ether moieties and salt effects for polymerization. *Polymer Journal* **2021,** *53* (9), 1057-1060.
(63) Chen, S.-Y.; Pan, R.-C.; Liu, Y.; Lu, X.-B., Bulky o-Phenylene-Bridged Bimetallic α-Diimine Ni (II) and Pd (II) Catalysts in Ethylene (Co) polymerization. *Organometallics* **2021,** *40* (22), 3703-3711.
(64) Dai, S.; Li, G.; Lu, W.; Liao, Y.; Fan, W., Suppression of chain transfer via a restricted rotation effect of dibenzosuberyl substituents in polymerization catalysis. *Polym. Chem* **2021,** *12* (22), 3240-3249.

(65) Ge, Y.; Li, S.; Fan, W.; Dai, S., Flexible "Sandwich"(8-Alkylnaphthyl α-Diimine) Catalysts in Insertion Polymerization. *Inorg. Chem.* **2021,** *60* (8), 5673-5681.
(66) Ge, Y.; Li, S.; Wang, H.; Dai, S., Synthesis of Branched Polyethylene and Ethylene-MA Copolymers Using Unsymmetrical Iminopyridyl Nickel and Palladium Complexes. *Organometallics* **2021,** *40* (17), 3033-3041.
(67) Guo, L.; Hu, X.; Lu, W.; Xu, G.; Liu, Q.; Dai, S., Investigations of ligand backbone effects on bulky diarylmethyl-based nickel (II) and palladium (II) catalyzed ethylene polymerization and copolymerization. *J. Organomet. Chem.* **2021,** *952*, 122046.
(68) Hai, Z.; Lu, Z.; Li, S.; Cao, Z.-Y.; Dai, S., The synergistic effect of rigid and flexible substituents on insertion polymerization with α-diimine nickel and palladium catalysts. *Polym. Chem* **2021,** *12* (32), 4643-4653.
(69) Li, S.; Dai, S., Highly efficient incorporation of polar comonomers in copolymerizations with ethylene using iminopyridyl palladium system. *J. Catal.* **2021,** *393*, 51-59.
(70) Liu, Y. S.; Harth, E., Distorted Sandwich α-Diimine PdII Catalyst: Linear Polyethylene and Synthesis of Ethylene/Acrylate Elastomers. *Angew. Chem. Int. Ed.* **2021**.
(71) Lu, W.; Xu, G.; Chang, G.; Wang, H.; Dai, S., Synthesis of highly branched polyethylene and ethylene-MA copolymers using hybrid bulky α-diimine Pd (II) catalysts. *J. Organomet. Chem.* **2021,** *956*, 122118.
(72) Wang, G.; Peng, D.; Sun, Y.; Chen, C., Interplay of supramolecular chemistry and photochemistry with palladium-catalyzed ethylene polymerization. *CCS Chemistry* **2021,** *3* (7), 2025-2034.
(73) Wang, X.-l.; Zhang, Y.-p.; Wang, F.; Pan, L.; Wang, B.; Li, Y.-s., Robust and Reactive Neutral Nickel Catalysts for Ethylene Polymerization and Copolymerization with a Challenging 1,1-Disubstituted Difunctional Polar Monomer. *ACS Catal.* **2021**, 2902-2911.
(74) Xia, J.; Han, Y.-F.; Kou, S.; Zhang, Y.; Jian, Z., Exploring steric effect of electron-donating group in palladium and nickel mediated ethylene polymerization and copolymerization with polar monomers. *European Polymer Journal* **2021,** *160*, 110781.
(75) Zhu, N.; Liang, T.; Huang, Y.; Pang, W.; Chen, M.; Tan, C., Influences of ligand backbone substituents on phosphinecarbonylpalladium and-nickel catalysts for ethylene polymerization and copolymerization with polar monomers. *Inorg. Chem.* **2021,** *60* (17), 13080-13090.
(76) Alberoni, C.; D'Alterio, M. C.; Balducci, G.; Immirzi, B.; Polentarutti, M.; Pellecchia, C.; Milani, B., Tunable "In-Chain" and "At the End of the Branches" Methyl Acrylate Incorporation in the Polyolefin Skeleton through Pd (II) Catalysis. *ACS Catal.* **2022,** *12* (6), 3430-3443.
(77) Liang, T.; Goudari, S. B.; Chen, C., A simple and versatile nickel platform for the generation of branched high molecular weight polyolefins. *Nat. Commun.* **2020,** *11* (1), 1-8.